# Collaborative Null-Steering Beamforming for Uniformly Distributed Wireless Sensor Networks

Keyvan Zarifi, *Member, IEEE*, Sofiène Affes, *Senior Member, IEEE*, and Ali Ghrayeb, *Senior Member, IEEE*

***Abstract*—Null-steering transmit beamformers aim to maximize the received signal power in the direction of the intended receiver while substantially reducing the power impinging on the unintended receivers located in other directions. The existing null-steering beamformers may not be directly applied in wireless sensor networks (WSNs) as they do not conform with the decentralized nature of WSNs and require every node to be aware of the locations of all other nodes in the network. This manuscript presents a novel collaborative null-steering beamformer that can be implemented in uniformly distributed WSNs in which each node is oblivious of other nodes' locations. The average beampattern expression of the proposed beamformer is derived and it is shown that the beampattern associated with any arbitrary realization of the nodes' locations converges with probability one to the so-obtained average beampattern as the number of collaborating nodes grows large. Properties of the average beampattern are analytically studied. In particular, it is proven that the average gain of the proposed beamformer is inversely proportional to the number of collaborating nodes in the directions of unintended receivers and further, if a mild condition is satisfied, it is approximately equal to that of the collaborative conventional beamformer in the directions with far angular distance from any unintended receiver.**

**It is argued that if virtual unintended receivers are assumed at proper directions, then the proposed collaborative null-steering beamformer can form an average beampattern with sidelobe peaks substantially smaller than those of the average beampattern of the collaborative conventional beamformer. To substantiate this argument, the optimal direction of a virtual unintended receiver is obtained such that its associated collaborative null-steering beamformer forms an average beampattern with minimal largest sidelobe peak. Depending on the number of collaborating nodes, it is further shown that the largest average sidelobe peak of the latter beamformer is up to 6.6 (dB) less than that of the collaborative conventional beamformer.**

***Index Terms*—Beampattern, collaborative beamforming, null-steering beamforming, wireless sensor networks.**

## I. Introduction

BORROWED from the literature of array processing for centralized antennas, collaborative beamforming for wireless sensor networks (WSNs) is a strong means to establish a reliable and energy-efficient communication link between small battery-powered sensor nodes and a distant access point (AP) that may be located far beyond the transmission range of each individual node [1]–[12]. This long-distance communication link is established by having a set of collaborating nodes simultaneously transmit properly weighted versions of a common data such that their radiated energies are constructively combined in the direction of the AP. Using $K$ collaborating nodes while fixing their total transmission power, the collaborative beamforming can result in up to $K$-fold gain in the received power at the AP [3], [6], [12]. As such, not only the nodes aggregate transmission range is substantially increased in the intended direction, but also each collaborating node can decrease its transmission power inversely proportional to $K$ to preserve its valuable limited energy resource.

Due to its practically appealing properties, collaborative beamforming for WSNs is a subject of an increasing attention in the research community. Assuming that the WSN nodes are uniformly distributed on a disc, a collaborative beamforming technique has been proposed in [1] and different characteristics of its resultant beampattern have been analyzed. Beampattern characteristics of the collaborative beamforming have also been investigated in details in [2] in the case that the collaborating nodes are distributed according to a two-dimensional Gaussian process. The application of collaborative beamforming has been extended in [3] to ad hoc WSNs wherein multiple concurrent source-destination pairs are present. How to select the collaborating nodes to achieve improved beampattern and network connectivity properties has been discussed in [4] and a heuristic algorithm to select the collaborating nodes that obtain a reasonable beamforming performance in the presence of nodes synchronization errors has been proposed in [5]. Robustness of the collaborative beamforming performance against the nodes asynchrony has been studied and a technique to synchronize the nodes has been presented in [6]. A carrier phase synchronization approach has been proposed in [7] to facilitate the implementation of collaborative beamforming in WSNs and convergence properties of a synchronization scheme for collaborative beamforming has been analyzed in [8]. Different beamforming techniques under partial channel state information and energy resource constraints are offered in [9]–[11]. A review on the collaborative beamforming techniques and the required synchronization approaches has been presented in [12].

In spite of their significant contributions, none of the above papers offer any specific treatment in the case where the AP is neighbored by unintended terminals that should be prevented from receiving the transmitted data. In many practical scenarios, however, not only is it required to increase the received power at the AP, but also it is crucial to avoid inducing interference on

Manuscript received May 15, 2009; accepted October 09, 2009. First published November 10, 2009; current version published February 10, 2010. The associate editor coordinating the review of this manuscript and approving it for publication was Dr. Ut-Va Koc. This work was supported in part by NSERC under grant N00858, a Canada research chair in high-speed wireless communications, the strategic partnership grants program of NSERC, and the NSERC postdoctoral fellowships program.

K. Zarifi is with Institut National de la Recherche Scientifique-Énergie, Matériaux, et Télécommunications (INRS-EMT), Université du Québec, Montreal, QC, H5A 1K6, Canada, and Concordia University, Montreal, QC, Canada (e-mail: zarifi@ieee.org).

S. Affes is with INRS-EMT, Université du Québec Montreal, QC, H5A 1K6, Canada (e-mail: affes@emt.inrs.ca).

A. Ghrayeb is with Concordia University, Montreal, QC, H3G 1M8, Canada (e-mail: aghrayeb@ece.concordia.ca).

Digital Object Identifier 10.1109/TSP.2009.2036476

undesired receiving terminals or to prevent intercepting terminals from recovering the transmitted signal. Proposed for centralized antenna arrays, the null-steering beamformer [13]–[18] accomplishes the above tasks by setting the antenna transmission weights such that while the transmitted signals are being constructively combined in the direction of the AP, they are deconstructively mixed in the directions of unintended receivers to the level at which no signal can be sensed in the latter directions. Depending on the application, this can substantially improve the network security against the intercepting terminals and/or increase the signal-to-interference-plus-noise ratio (SINR) at the undesired receiving terminals by decreasing their interference level. Although a wide range of applications in WSNs can significantly benefit from a reduced signal energy in the directions of unintended receivers, to the best of our knowledge, there has been no attempt to apply the null-steering beamforming technique in WSNs.

In this paper, we present a null-steering beamforming technique tailored for distributed WSNs. We start with identifying the main challenge in adopting the null-steering beamformer from the centralized array processing literature to the context of WSNs. We show that the classic form of the null-steering beamformer may not be directly applied in WSNs as it requires that the exact locations of all nodes to be globally available at every node; a requirement that does not conform with the distributed nature of WSNs and, moreover, is not scalable as the number of collaborating nodes $K$ grows large. We assume that the collaborating nodes are uniformly distributed on a disc of an arbitrary radius [1], [3], [19]–[22] and use this statistical information to introduce a novel collaborative null-steering beamformer that is applicable in WSNs in which each node is oblivious of all other nodes' locations. The average beampattern expression of the proposed collaborative null-steering beamformer is obtained and it is further proved that any arbitrary realization of the collaborating nodes' locations results in a beampattern that converges with probability one to the so-obtained average beampattern as $K$ grows large. Different properties of the average beampattern are analyzed in details. In particular, it is proven that the average gain of the proposed collaborative null-steering beamformer is inversely proportional to $K$ in the directions of unintended receivers. Moreover, it is shown that if the angular distances between the AP and the unintended receivers are not very small and the radius of the disc that includes the collaborating nodes is large enough, then the average gain of the proposed beamformer is approximately equal to that of the collaborative conventional beamformer [1] in directions with an angular distance far enough from any unintended receiver.

Assuming virtual unintended receivers with adjustable angular locations, it is demonstrated that the null positions may be treated as design parameters that can be tuned to form an average beampattern with sidelobe peaks considerably smaller than those of the average beampattern of the collaborative conventional beamformer in [1]. To this end, a collaborative null-steering beamformer is designed whose single null is optimally positioned to minimize the maximum sidelobe of the average beampattern while inducing a negligible degradation to the received power at the AP.

The rest of the paper is organized as follows. Section II presents the signal model and Section III proposes the collaborative null-steering beamformer. The average beampattern of the proposed collaborative null-steering beamformer is analyzed in Section IV and a collaborative null-steering beamformer with optimal sidelobe properties is designed in Section V. Simulated examples are used in Section VI to validate the analytical results of Section IV and the efficiency of the design approach of Section V. Concluding remarks are given in Section VII.

*Notation:* Uppercase and lowercase bold letters denote matrices and vectors, respectively. $[\cdot]_{il}$, $[\cdot]_{\cdot,l}$, and $[\cdot]_i$ are the $(i,l)$th entry of a matrix, $l$th column of a matrix, and $i$th entry of a vector, respectively. $j \triangleq \sqrt{-1}$, $\mathbf{I}$ is the identity matrix, and $\mathbf{e}_i$ is a vector with one in the $i$th position and zeros elsewhere. $(\cdot)^T$, $(\cdot)^*$, and $(\cdot)^H$ denote the transpose, the conjugate, and the Hermitian transpose, respectively. $\|\cdot\|$ is the 2-norm of a vector and $|\cdot|$ is the absolute value. $\mathrm{E}\{\cdot\}$ stands for the statistical expectation and $(\xrightarrow{ep1})$ $\xrightarrow{p1}$ denotes (element-wise) convergence with probability one. $J_n(\cdot)$ stands for the $n$th order Bessel function of the first kind.

## II. System Model

The geometrical structure of the WSN cluster and the receiver terminals are illustrated in Fig. 1 where $K$ cluster nodes are uniformly distributed on $D(O,R)$, the disc centered at $O$ with radius $R$ [1], [3], [19]–[22], while the cluster AP as well as $L < K$ unintended receivers are located in the same plane containing $D(O,R)$. Given a total transmission power budget, the cluster nodes form a virtual antenna array and collaboratively transmit a common message $z(t)$ aiming to simultaneously achieve the following two goals:

- **G1**: The received signal power at the AP is maximized.
- **G2**: The received signal powers at all unintended receivers are zero.

Without any loss of generality, let $O$ be the pole and the line connecting $O$ to the AP be the $x$ axis of a polar coordinate system. Denote the polar coordinates of the $k$th cluster node as $(r_k, \psi_k)$ and the polar coordinates of the AP and the unintended receivers as $(A_0, \phi_0 = 0)$ and $(A_l, \phi_l), l = 1, \ldots, L$, respectively. The following assumptions are adopted throughout this paper:

- **A1**: The AP as well as all unintended receivers are in the far-field of the WSN cluster such that

$$A_l \gg R, \quad l = 0, 1, \ldots, L. \tag{1}$$

- **A2**: The bandwidth of $z(t)$ is narrow enough such that $z(t)$ is almost constant during $2R/c$ seconds where $c$ is the speed of an electromagnetic wave.
- **A3**: The effect of signal reflection or scattering is negligible. Therefore, there is no multipath fading or shadowing.
- **A4**: All cluster nodes can be perfectly synchronized both in the carrier frequency and the initial phase.[1]
- **A5**: The $k$th node is only aware of its own coordinates $(r_k, \psi_k)$ and the directions of the receiving terminals $\phi_l, l = 0, 1, \ldots, L$, while being unaware of the locations of all other nodes as well as $A_l, l = 0, 1, \ldots, L$.

[1]A variety of synchronization techniques for WSNs have been developed in the literature (see, e.g., [3], [6]–[8]).

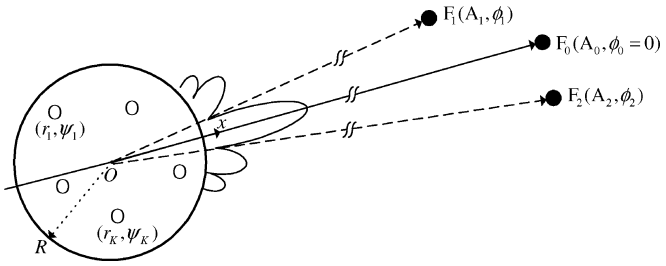


Fig. 1. The geometrical structure of the WSN cluster and the receiver terminals.

Assumptions **A1**–**A4** are common in the literature of array processing for planar waves [23]–[26] and are frequently adopted in the context of collaborative beamforming for WSNs [1]–[5], [12] while **A5** is due to the distributed and unsupervised characteristics of WSNs.

Let

$$s_k(t) = w_k^* z(t) e^{j2\pi ft} \tag{2}$$

denote the transmitted signal from the $k$th node where $z(t)$ is the modulating signal with $\mathrm{E}\{|z(t)|^2\} = 1, w_k^*$ is the $k$th node transmission weight, and $f$ is the carrier frequency. Using **A1** and **A3**, the received signal at an arbitrary point $F_\bullet(A_\bullet, \phi_\bullet)$ in the far-field due to the $k$th node transmission can be represented as

$$\begin{aligned} y_{F_\bullet,k}(t) &= \beta_{F_\bullet,k} s_k\left(t - \frac{d_{F_\bullet,k}}{c}\right) \\ &= \beta_{F_\bullet,k} w_k^* z\left(t - \frac{d_{F_\bullet,k}}{c}\right) e^{-j\frac{2\pi}{\lambda} d_{F_\bullet,k}} e^{j2\pi ft} \end{aligned} \tag{3}$$

where $d_{F_\bullet,k}$ is the distance between the $k$th node and $F_\bullet, \lambda$ is the carrier wavelength, and $\beta_{F_\bullet,k} = d_{F_\bullet,k}^{-\gamma/2}$ is the signal path loss with $\gamma$ denoting the path loss exponent. Note that

$$\begin{aligned} d_{F_\bullet,k} &= \left(A_\bullet^2 + r_k^2 - 2A_\bullet r_k \cos(\phi_\bullet - \psi_k)\right)^{1/2} \\ &\approx A_\bullet - r_k \cos(\phi_\bullet - \psi_k) \end{aligned} \tag{4}$$

where the approximate equality in the second line is due to (1). Substituting (4) in (3) and using **A2** to simplify the result, it follows that

$$\begin{aligned} y_{F_\bullet,k}(t) \approx \beta_{F_\bullet,k} e^{-j\frac{2\pi}{\lambda}A_\bullet} \\ \cdot z\left(t - \frac{A_\bullet}{c}\right) w_k^* e^{j\frac{2\pi}{\lambda} r_k \cos(\phi_\bullet - \psi_k)} e^{j2\pi ft}. \end{aligned} \tag{5}$$

We also obtain from (4) that

$$\begin{aligned} \beta_{F_\bullet,k} &\approx \left(A_\bullet - r_k \cos(\phi_\bullet - \psi_k)\right)^{-\gamma/2} \\ &\approx \beta_{F_\bullet}\left(1 + \frac{\gamma r_k \cos(\phi_\bullet - \psi_k)}{2A_\bullet}\right) \end{aligned} \tag{6}$$

where $\beta_{F_\bullet} \triangleq A_\bullet^{-\gamma/2}$. Due to (1), $\gamma r_k \cos(\phi_\bullet - \psi_k)/2A_\bullet \ll 1$ and we have $\beta_{F_\bullet,k} \approx \beta_{F_\bullet}$. The latter result implies that the path losses of the signals transmitted from all cluster nodes and received at a far-field point $F_\bullet$ can be assumed to be equal [1]–[4]. Let us introduce

$$\mathbf{a}_{\phi_\bullet} \triangleq \left[e^{j\frac{2\pi}{\lambda} r_1 \cos(\phi_\bullet - \psi_1)} \dots e^{j\frac{2\pi}{\lambda} r_K \cos(\phi_\bullet - \psi_K)}\right]^T \tag{7}$$

$$\mathbf{w} \triangleq [w_1 \dots w_K]^T. \tag{8}$$

The total received signal at $F_\bullet$ due to all cluster nodes is approximately given by

$$y_{F_\bullet}(t) = \beta_{F_\bullet} e^{-j\frac{2\pi}{\lambda}A_\bullet} z\left(t - \frac{A_\bullet}{c}\right) e^{j2\pi ft} \mathbf{w}^H \mathbf{a}_{\phi_\bullet}. \tag{9}$$

As such, the total received power at $F_\bullet$ can be computed as

$$\xi_{F_\bullet} = \beta_{F_\bullet}^2 |\mathbf{w}^H \mathbf{a}_{\phi_\bullet}|^2. \tag{10}$$

Let $\mathbf{A} \triangleq [\mathbf{a}_{\phi_1} \dots \mathbf{a}_{\phi_L}]$ and $P_T$ denote the maximum admissible total transmission power. It is direct to observe that **G1** and **G2** can be achieved if $\mathbf{w}$ is a solution to

$$\begin{aligned} &\max_{\mathbf{w}} |\mathbf{w}^H \mathbf{a}_0|^2 \\ &\text{subject to} \quad \begin{matrix} \mathbf{w}^H \mathbf{A} = \mathbf{0} \\ \mathbf{w}^H \mathbf{w} \le P_T \end{matrix}. \end{aligned} \tag{11}$$

Note that the optimal solution to (11) should satisfy the total transmission power constraint with equality as, otherwise, the so-obtained solution could be scaled up to have $\mathbf{w}^H \mathbf{w} = P_T$ while increasing the objective function. This immediately results in a contradiction to the optimality of such a solution. The optimal solution to (11) is given by

$$\mathbf{w}_{\mathrm{ns}} = \frac{\sqrt{P_T}}{\|(\mathbf{I} - \mathbf{P}_\mathbf{A})\,\mathbf{a}_0\|} \cdot (\mathbf{I} - \mathbf{P}_\mathbf{A})\,\mathbf{a}_0 \tag{12}$$

where

$$\mathbf{P}_\mathbf{A} \triangleq \mathbf{A}(\mathbf{A}^H \mathbf{A})^{-1} \mathbf{A}^H \tag{13}$$

is the orthogonal projection matrix onto the subspace spanned by the columns of $\mathbf{A}$. As such, $\mathbf{w}_{\mathrm{ns}}$ is in fact the orthogonal projection of $\mathbf{a}_0$ onto the null space of $\mathbf{A}$. In the array processing literature, the solution to (11) is sometimes called the null-steering beamformer [14]–[18]. This justifies the subscript of $\mathbf{w}_{\mathrm{ns}}$ as well as the title of this manuscript. Note that in the conventional scenario where there is no unintended receiver, $\mathbf{A} = \mathbf{0}$ and the solution to (11) reduces to the collaborative conventional beamformer

$$\mathbf{w}_{\mathrm{c}} = \sqrt{\frac{P_T}{K}} \mathbf{a}_0. \tag{14}$$

## III. Collaborative Null-Steering Beamformer

Let us define

$$\mathbf{E} \triangleq \frac{1}{K} \mathbf{A}^H \mathbf{A} \tag{15}$$

$$\mathbf{g}_{\phi_\bullet} \triangleq \frac{1}{K} \mathbf{A}^H \mathbf{a}_{\phi_\bullet}. \tag{16}$$

The null-steering beamformer (12) can be alternatively rewritten as

$$\mathbf{w}_{\rm ns} = \frac{\sqrt{P_T}}{\|\mathbf{a}_0 - \mathbf{A}\mathbf{E}^{-1}\mathbf{g}_0\|} \cdot (\mathbf{a}_0 - \mathbf{A}\mathbf{E}^{-1}\mathbf{g}_0) = \frac{\sqrt{P_T}}{\sqrt{K\left(1 - \mathbf{g}_0^H\mathbf{E}^{-1}\mathbf{g}_0\right)}} \cdot \left(\mathbf{a}_0 - \mathbf{A}\mathbf{E}^{-1}\mathbf{g}_0\right). \quad (17)$$

Equation (17) shows that **G1** and **G2** are simultaneously achieved subject to the total transmission power $P_T$ if

$$\begin{aligned} w_k &= [\mathbf{w}_{\rm ns}]_k \\ &= \frac{\sqrt{P_T}}{\sqrt{K\left(1 - \mathbf{g}_0^H\mathbf{E}^{-1}\mathbf{g}_0\right)}} \cdot \left([\mathbf{a}_0]_k - \sum_{i=1}^{L}[\mathbf{A}]_{ki}[\mathbf{E}^{-1}\mathbf{g}_0]_i\right) \\ &= \frac{\sqrt{P_T}}{\sqrt{K\left(1 - \mathbf{g}_0^H\mathbf{E}^{-1}\mathbf{g}_0\right)}} \cdot \left(e^{j\frac{2\pi}{\lambda}r_k\cos(\phi_0-\psi_k)} - \sum_{i=1}^{L} e^{j\frac{2\pi}{\lambda}r_k\cos(\phi_i-\psi_k)}[\mathbf{E}^{-1}\mathbf{g}_0]_i\right). \end{aligned} \quad (18)$$

Note from (18) that the null-steering beamformer (17) can be implemented only when the $k$th node ($k = 1,\ldots,K$) knows all $e^{j(2\pi/\lambda)r_k\cos(\phi_i-\psi_k)}$ for $i = 0,\ldots,L$ as well as all entries of the $L \times L$ matrix $\mathbf{E}$ and the $L \times 1$ vector $\mathbf{g}_0$. It follows from **A5** that the $k$th node can use its available knowledge to obtain $e^{j(2\pi/\lambda)r_k\cos(\phi_i-\psi_k)}, i = 0,\ldots,L$. However, this knowledge is not sufficient to obtain $\mathbf{E}$ and $\mathbf{g}_0$. In fact, it is straightforward to verify that $\mathbf{E}$ and $\mathbf{g}_0$ depend on the locations of all the cluster nodes. Therefore, $\mathbf{w}_{\rm ns}$ can be implemented only if every node knows the exact locations of all nodes in the cluster. Unfortunately, this requirement does not conform with **A5**.

To get around this problem and be able to implement (an approximate) null-steering beamformer in a distributed fashion, one needs to substitute $\mathbf{E}$ and $\mathbf{g}_0$ in (17) with other quantities that are endowed with the following two properties:

- **P1:** The substituting quantities are good approximations of their original counterparts.
- **P2:** Entries of the substituting quantities depend only on the parameters *commonly* known at every node, that is, $\phi_l, l = 0,1,\ldots,L$.

In light of the facts that the total transmission power from the whole network is constrained to $P_T$ and each collaborating node has a limited nonrenewable energy resource, it makes practical sense to use a large number of nodes in our collaborative beamforming scheme in return to a low transmission power from each individual node. For scenarios with a large $K$, $\lim_{K\to\infty}\mathbf{E}$ and $\lim_{K\to\infty}\mathbf{g}_0$ can serve as accurate approximations of $\mathbf{E}$ and $\mathbf{g}_0$, respectively. However, to be able to use $\lim_{K\to\infty}\mathbf{E}$ and $\lim_{K\to\infty}\mathbf{g}_0$ in lieu of $\mathbf{E}$ and $\mathbf{g}_0$, we require to verify that the approximating quantities also satisfy **P2**.

Note from (15) and (16) that

$$[\mathbf{E}]_{mn} = \frac{1}{K}\mathbf{a}_{\phi_m}^H\mathbf{a}_{\phi_n} \quad (19)$$

$$[\mathbf{g}_0]_m = \frac{1}{K}\mathbf{a}_{\phi_m}^H\mathbf{a}_0. \quad (20)$$

Equations (19) and (20) show that $\lim_{K\to\infty}\mathbf{E}$ and $\lim_{K\to\infty}\mathbf{g}_0$ entirely depend on $\lim_{K\to\infty}\mathbf{a}_{\phi_m}^H\mathbf{a}_{\phi_n}$. The following theorem on asymptotic properties of $\mathbf{a}_{\phi_m}^H\mathbf{a}_{\phi_n}$ is essential in our later developments.

*Theorem 1:* Consider $\mathbf{a}_{\phi_\bullet}$ as defined in (7). Assuming that the nodes are uniformly distributed on $D(O,R)$, we have for $m = 1,\ldots,L$ and $n = 0,1,\ldots,L$ that

$$\frac{1}{K}\mathbf{a}_{\phi_m}^H\mathbf{a}_{\phi_n} = \frac{1}{K}\sum_{k=1}^{K} e^{j\alpha(\phi_n-\phi_m)z_k} \quad (21)$$

where $\alpha(\phi_\bullet) \triangleq 4\pi\tilde{R}\sin(\phi_\bullet/2)$ and $\tilde{R} \triangleq R/\lambda$. Moreover,

$$z_k \triangleq \frac{r_k}{R}\cdot\sin\left(\psi_k - \frac{\phi_n+\phi_m}{2}\right) \qquad k = 1,\ldots,K \quad (22)$$

are independent and identically distributed (i.i.d.) random variables with the following probability density function (PDF):

$$f_{z_k}(z) = \frac{2}{\pi}\sqrt{1-z^2} \quad z_k \in [-1,1]. \quad (23)$$

We have

$$\frac{1}{K}\mathrm{E}\left\{\mathbf{a}_{\phi_m}^H\mathbf{a}_{\phi_n}\right\} = \mathrm{E}\left\{e^{j\alpha(\phi_n-\phi_m)z_k}\right\} = \begin{cases} \frac{2}{\alpha(\phi_n-\phi_m)}J_1(\alpha(\phi_n-\phi_m)) & m \neq n \\ 1 & m = n \end{cases}. \quad (24)$$

Moreover, it holds that

$$\lim_{K\to\infty}\frac{1}{K}\mathbf{a}_{\phi_m}^H\mathbf{a}_{\phi_n} \xrightarrow{p1} \frac{1}{K}\sum_{k=1}^{K}\mathrm{E}\left\{e^{j\alpha(\phi_n-\phi_m)z_k}\right\} = \begin{cases} \frac{2}{\alpha(\phi_n-\phi_m)}J_1(\alpha(\phi_n-\phi_m)) & m \neq n \\ 1 & m = n \end{cases}. \quad (25)$$

*Proof:* See Appendix A. □

Note that as $\psi_k$ is uniformly distributed on $[-\pi,\pi)$, the fixed bias of $-(\phi_n+\phi_m)/2$ in the argument of $\sin(\cdot)$ in the RHS of (22) does not have any effect on the PDF of $z_k$.

Using (24) and (25) in (19) and (20), we obtain the following result.

*Corollary 1:* Consider the $L \times L$ matrix $\bar{\mathbf{E}}$ and the $L \times 1$ vector $\bar{\mathbf{g}}_0$ with

$$[\bar{\mathbf{E}}]_{mn} \triangleq \begin{cases} \frac{2}{\alpha(\phi_n-\phi_m)}J_1(\alpha(\phi_n-\phi_m)) & m \neq n \\ 1 & m = n \end{cases} \quad (26)$$

$$[\bar{\mathbf{g}}_0]_m \triangleq \frac{2}{\alpha(\phi_m)}J_1(\alpha(\phi_m)). \quad (27)$$

We have

$$\lim_{K\to\infty}\mathbf{E} \xrightarrow{ep1} \mathrm{E}\{\mathbf{E}\} = \bar{\mathbf{E}} \quad (28)$$

$$\lim_{K\to\infty}\mathbf{g}_0 \xrightarrow{ep1} \mathrm{E}\{\mathbf{g}_0\} = \bar{\mathbf{g}}_0. \quad (29)$$

Corollary 1 shows that the entries of $\lim_{K\to\infty}\mathbf{E}$ and $\lim_{K\to\infty}\mathbf{g}_0$ converge with probability one to values that exclusively depend on $\alpha(\phi_n-\phi_m), m = 1,\ldots,L, n = 0,1\ldots,L$. As $\alpha(\phi_n-\phi_m)$ depends solely on $\phi_n-\phi_m$, it follows that

entries of both $\lim_{K\to\infty}\mathbf{E}$ and $\lim_{K\to\infty}\mathbf{g}_0$ satisfy **P2**. Therefore, we propose to use

$$\bar{\mathbf{w}}_{\rm NS}=\frac{\sqrt{P_T}}{\sqrt{K\left(1-\bar{\mathbf{g}}_0^H\bar{\mathbf{E}}^{-1}\bar{\mathbf{g}}_0\right)}}\cdot(\mathbf{a}_0-\mathbf{A}\bar{\mathbf{E}}^{-1}\bar{\mathbf{g}}_0). \tag{30}$$

in lieu of $\mathbf{w}_{\rm NS}$. Note that $\bar{\mathbf{w}}_{\rm NS}$ accurately approximates the null-steering beamformer $\mathbf{w}_{\rm NS}$ for a large $K$, and, in addition, can be collaboratively implemented by nodes in a distributed fashion. It also directly follows from (28)–(30) that

$$\lim_{K\to\infty}\bar{\mathbf{w}}_{\rm NS}^H\bar{\mathbf{w}}_{\rm NS}\xrightarrow{ep1}\mathrm{E}\left\{\bar{\mathbf{w}}_{\rm NS}^H\bar{\mathbf{w}}_{\rm NS}\right\}=P_T. \tag{31}$$

As such, the proposed collaborative null-steering beamformer satisfies the total transmission power constraint both in average and in the asymptotic case of large $K$. It is worth mentioning that a relevant approach to the above technique has been used before to develop transmission techniques that rely on available statistical channel state information (CSI) in lieu of an unknown instantaneous CSI (see, e.g., [11], [27]–[30]).

Assume that the collaborative null-steering beamformer $\bar{\mathbf{w}}_{\rm NS}$ is used in the WSN cluster. As follows from (10), the received power at an arbitrary point $F_\bullet(A_\bullet,\phi_\bullet)$ in the far-field is given by

$$\xi_{F_\bullet}=KP_T\beta_{F_\bullet}^2P(\phi_\bullet|\mathbf{z}) \tag{32}$$

where

$$\begin{aligned}P(\phi_\bullet|\mathbf{z})&\triangleq\frac{1}{KP_T}\left|\bar{\mathbf{w}}_{\rm NS}^H\mathbf{a}_{\phi_\bullet}\right|^2\\&=\frac{\left|\left(\mathbf{a}_0-\mathbf{A}\bar{\mathbf{E}}^{-1}\bar{\mathbf{g}}_0\right)^H\mathbf{a}_{\phi_\bullet}\right|^2}{K^2\left(1-\bar{\mathbf{g}}_0^T\bar{\mathbf{E}}^{-1}\bar{\mathbf{g}}_0\right)}\end{aligned} \tag{33}$$

is called the far-field beampattern and $\mathbf{z}\triangleq[z_1,\ldots,z_K]$ is used in (33) to stress the fact that $P(\phi_\bullet|\mathbf{z})$ is a random variable that depends on the entries of $\mathbf{z}$. Note that $1/KP_T$ in the first line of (33) is a scaling factor used to follow the common practice to have $P(\phi_0=0|\mathbf{z})=1$ in the conventional case where there is no unintended receiver and $\bar{\mathbf{w}}_{\rm NS}$ simplifies to (14).

As $P(\phi_\bullet|\mathbf{z})$ is a function of $\mathbf{z}$, analyzing the properties of the average beampattern

$$\tilde{P}(\phi_\bullet)\triangleq\mathrm{E}_{\mathbf{z}}\{P(\phi_\bullet|\mathbf{z})\} \tag{34}$$

as well as the values of $\tilde{P}(\phi_\bullet)$ at $\phi_\bullet=\phi_l, l=0,1,\ldots,L$ (commonly known as the average gain of the beamformer at $\phi_\bullet=\phi_l, l=0,1,\ldots,L$) are of significant importance. Section IV investigates the properties of $\tilde{P}(\phi_\bullet)$ and proves that as the number of nodes $K$ grows larger, $P(\phi_\bullet|\mathbf{z})$ converges to $\tilde{P}(\phi_\bullet)$ for any arbitrary realization of $\mathbf{z}$. This further justifies the practical importance of $\tilde{P}(\phi_\bullet)$.

## IV. Properties of the Average Beampattern

### A. Average Beampattern Expression

The main result of this section is given in the following theorem.

*Theorem 2:* Assuming that the collaborative null-steering beamformer (30) is used, we have

$$\begin{aligned}\tilde{P}(\phi_\bullet)=&\frac{1}{K}+\left(1-\frac{1}{K}\right)\cdot\frac{1}{1-\bar{\mathbf{g}}_0^T\bar{\mathbf{E}}^{-1}\bar{\mathbf{g}}_0}\\&\cdot\left(\frac{2}{\alpha(\phi_\bullet)}J_1\left(\alpha(\phi_\bullet)\right)-\bar{\mathbf{g}}_0^T\bar{\mathbf{E}}^{-1}\bar{\mathbf{g}}_{\phi_\bullet}\right)^2\end{aligned} \tag{35}$$

where $\bar{\mathbf{g}}_{\phi_\bullet}$ is an $L\times 1$ vector with

$$[\bar{\mathbf{g}}_{\phi_\bullet}]_l\triangleq\begin{cases}\frac{2}{\alpha(\phi_\bullet-\phi_l)}J_1(\alpha(\phi_\bullet-\phi_l)) & \phi_\bullet\neq\phi_l\\ 1 & \phi_\bullet=\phi_l\end{cases}. \tag{36}$$

moreover, it holds for any arbitrary realization of $\mathbf{z}$ that

$$\begin{aligned}\lim_{K\to\infty}P(\phi_\bullet|\mathbf{z})\xrightarrow{p1}\lim_{K\to\infty}\tilde{P}(\phi_\bullet)=&\frac{1}{1-\bar{\mathbf{g}}_0^T\bar{\mathbf{E}}^{-1}\bar{\mathbf{g}}_0}\\&\cdot\left(\frac{2}{\alpha(\phi_\bullet)}J_1(\alpha(\phi_\bullet))-\bar{\mathbf{g}}_0^T\bar{\mathbf{E}}^{-1}\bar{\mathbf{g}}_{\phi_\bullet}\right)^2.\end{aligned} \tag{37}$$

*Proof:* See Appendix B. □

As can be observed from (35), $\tilde{P}(\phi_\bullet)$ is comprised of two terms: 1) The first term of $1/K$ that is independent of $\phi_\bullet$ and diminishes to zero as $K$ grows large. This term merely determines the floor level of the average beampattern curve; 2) The second term that depends on $\phi_\bullet$, is nonnegative (see Section IV-C), and does not converge to zero as $K$ grows large. This term determines the shape of the average beampattern curve. In particular, the minimum and the peak points of the average beampattern sidelobe are the roots and the maximum points of this term, respectively.

Note from (37) that, when $K$ is large enough, $\tilde{P}(\phi_\bullet)$ is a reliable approximation of $P(\phi_\bullet|\mathbf{z})$ for any arbitrary realization of $\mathbf{z}$ and both above quantities are well-approximated by the limiting value of the second term in the RHS of (35).

The following discussions on the properties of $\tilde{P}(\phi_\bullet)$ are also in order.

### B. Average Gain at $\phi_l$

To examine the effectiveness of $\bar{\mathbf{w}}_{\rm NS}$ in reducing the received signal power at $\phi_l, l=1,\ldots,L$, let us obtain

$$\begin{aligned}\tilde{P}(\phi_l)=&\frac{1}{K}+\left(1-\frac{1}{K}\right)\cdot\frac{1}{1-\bar{\mathbf{g}}_0^T\bar{\mathbf{E}}^{-1}\bar{\mathbf{g}}_0}\\&\cdot\left(\frac{2}{\alpha(\phi_l)}J_1(\alpha(\phi_l))-\bar{\mathbf{g}}_0^T\bar{\mathbf{E}}^{-1}\bar{\mathbf{g}}_{\phi_l}\right)^2.\end{aligned} \tag{38}$$

Note from (26) and (36) that

$$\bar{\mathbf{g}}_l=\bar{\mathbf{E}}_{\cdot,l}=\bar{\mathbf{E}}\mathbf{e}_l. \tag{39}$$

Using (39) in (38) yields

$$\begin{aligned}\tilde{P}(\phi_l)=&\frac{1}{K}+\left(1-\frac{1}{K}\right)\cdot\frac{1}{1-\bar{\mathbf{g}}_0^T\bar{\mathbf{E}}^{-1}\bar{\mathbf{g}}_0}\\&\cdot\left(\frac{2}{\alpha(\phi_l)}J_1(\alpha(\phi_l))-\bar{\mathbf{g}}_0^T\mathbf{e}_l\right)^2\\=&\frac{1}{K}\end{aligned} \tag{40}$$

for $l = 1, \ldots, L$. Equation (40) shows that $\phi_l, l = 1, \ldots, L$, are in fact the minimum points of the average beampattern. It can also be observed from the latter equation that the price of using $\bar{\mathbf{w}}_{\mathrm{ns}}$ in lieu of $\mathbf{w}_{\mathrm{ns}}$ is to elevate the minimum levels at $\phi_l, l = 1, \ldots, L$ from zero to $1/K$. Note that, as $K$ grows large, $\bar{\mathbf{w}}_{\mathrm{ns}}$ converges to $\mathbf{w}_{\mathrm{ns}}$ and $1/K$ diminishes to zero. It is also worth recalling that, as $K$ increases, $P(\phi_\bullet|\mathbf{z})$ converges to $\tilde{P}(\phi_\bullet)$ regardless of the realization of $\mathbf{z}$. Therefore, $\phi_l, l = 1, \ldots, L$ are not only the minimum points of $\tilde{P}(\phi_\bullet)$ for a bounded $K$, but also the nulls of $P(\phi_\bullet|\mathbf{z})$ for any arbitrary realization of the nodes' locations in the asymptotic regime of a large $K$.

### C. Average Gain in the Direction of the AP

The fact that

$$\lim_{\phi_\bullet \to 0} \frac{2}{\alpha(\phi_\bullet)} J_1(\alpha(\phi_\bullet)) = 1 \tag{41}$$

can be used in (35) to obtain

$$\tilde{P}(0) = 1 - \bar{\mathbf{g}}_0^T \bar{\mathbf{E}}^{-1} \bar{\mathbf{g}}_0 + \frac{1}{K} \bar{\mathbf{g}}_0^T \bar{\mathbf{E}}^{-1} \bar{\mathbf{g}}_0. \tag{42}$$

Equation (42) shows that $\tilde{P}(0)$ entirely depends on $K$ and $\bar{\mathbf{g}}_0^T \bar{\mathbf{E}}^{-1} \bar{\mathbf{g}}_0$. It can be observed from (15), (16), (28), (29) as well as the definition of $\mathbf{P}_{\mathbf{A}}$ in (13) that

$$\lim_{K \to \infty} \frac{1}{K} \|\mathbf{P}_{\mathbf{A}} \mathbf{a}_0\|^2 \xrightarrow{p1} \bar{\mathbf{g}}_0^T \bar{\mathbf{E}}^{-1} \bar{\mathbf{g}}_0. \tag{43}$$

As $\|\mathbf{P}_{\mathbf{A}} \mathbf{a}_0\|$ is the length of the orthogonal projection of $\mathbf{a}_0$ onto the column span of $\mathbf{A}$, we have $\|\mathbf{P}_{\mathbf{A}} \mathbf{a}_0\| \leq \|\mathbf{a}_0\|$, and, therefore,

$$0 \leq \frac{1}{K} \|\mathbf{P}_{\mathbf{A}} \mathbf{a}_0\|^2 \leq 1 \tag{44}$$

where the left-hand side (LHS) inequality holds with equality if $\mathbf{a}_0$ is orthogonal to the column span of $\mathbf{A}$ and the RHS inequality holds with equality if $\mathbf{a}_0$ is in the column span of $\mathbf{A}$. It follows from (43) and (44) that $\bar{\mathbf{g}}_0^T \bar{\mathbf{E}}^{-1} \bar{\mathbf{g}}_0 \in [0, 1]$. Note from (42) that $\tilde{P}(0)$ is a decreasing function of $\bar{\mathbf{g}}_0^T \bar{\mathbf{E}}^{-1} \bar{\mathbf{g}}_0$ in the latter interval and, as $\bar{\mathbf{g}}_0^T \bar{\mathbf{E}}^{-1} \bar{\mathbf{g}}_0$ increases from 0 to 1, $\tilde{P}(0)$ decreases from 1 to 0. It should be mentioned that the decrease in $\tilde{P}(0)$ is the price that may have to be paid for devising minimum points in the directions of unintended receivers. In fact, as $\bar{\mathbf{w}}_{\mathrm{ns}}$ is derived such that $|\bar{\mathbf{w}}_{\mathrm{ns}}^H \mathbf{a}_{\phi_l}| \approx 0, l = 1, \ldots, L$, the more $\mathbf{a}_0$ leans towards the column span of $\mathbf{A}$, the smaller the $|\bar{\mathbf{w}}_{\mathrm{ns}}^H \mathbf{a}_0|$, and, consequently, the more the decrease in $\tilde{P}(0)$. Note that a similar property also holds for the null-steering beamformer in the array processing literature for centralized antennas. We show in Section IV-F that, under a mild condition, $\bar{\mathbf{g}}_0^T \bar{\mathbf{E}}^{-1} \bar{\mathbf{g}}_0 \approx 0$ and therefore suppressing the received signal power in the directions of unintended receivers has a negligible impact on $\tilde{P}(0)$.

Note from (32) that the average received power at an arbitrary point $F_\bullet(A_\bullet, \phi_\bullet)$ in the far-field is given by

$$\tilde{\xi}_{F_\bullet} = \mathrm{E}_{\mathbf{z}}\{\xi_{F_\bullet}\} = K P_T \beta_{F_\bullet}^2 \tilde{P}(\phi_\bullet). \tag{45}$$

It follows from (42) and (45) that the average received power at the AP can be computed as

$$\tilde{\xi}_{F_0} \approx K P_T \beta_{F_0}^2 \left(1 - \bar{\mathbf{g}}_0^T \bar{\mathbf{E}}^{-1} \bar{\mathbf{g}}_0\right) \tag{46}$$

while, according to (40) and (45), the average received power at the unintended receivers is equal to

$$\tilde{\xi}_{Fl} = P_T \beta_{F_0}^2 \quad l = 1, \ldots, L. \tag{47}$$

As such, while the average received power at the AP increases proportionally to the number of collaborating nodes $K$, the average received power at the unintended receivers does not increase with $K$ and is given by $P_T \beta_{F_0}^2$; the power that would have been received if only a single node were to transmit its signal. Therefore, as the unintended receivers are assumed to be in the far-field and typically far beyond the transmission range of any individual node, the proposed collaborative null-steering beamformer is able to guarantee the information security against the intercepting terminals and/or increase the SINR of the undesired receivers through containing their interferences below a negligible level. It is also worth mentioning that if the term $\gamma r_k \cos(\phi_\bullet - \psi_k)/2A_\bullet$ is not ignored in (6), then the resulting average received power expression at $F_\bullet$ differs from $\tilde{\xi}_{F_\bullet}$ only by a value that is proportional to $(R/A_\bullet)^2$ ([3], Section IV-C). This further verifies the accuracy of the equal path loss approximation $\beta_{F_\bullet} \approx \beta_{F_\bullet,k}, k = 1, \ldots, K$.

### D. Average Beampattern for $L = 0$

Similar to $\mathbf{w}_{\mathrm{ns}}, \bar{\mathbf{w}}_{\mathrm{ns}}$ also reduces to the collaborative conventional beamformer (14) if there is no unintended receiver ($L = 0$). In such a case, it is direct to show that $\tilde{P}(\phi_\bullet)$ in (35) boils down to

$$\tilde{P}_{\mathrm{c}}(\phi_\bullet) = \frac{1}{K} + \left(1 - \frac{1}{K}\right) \left(\frac{2}{\alpha(\phi_\bullet)} J_1(\alpha(\phi_\bullet))\right)^2. \tag{48}$$

The same expression as in (48) has been obtained before in [1] for the conventional scenario in which the AP is the only receiving terminal. As can be observed from (48), since $L = 0$ and there is no devised minima, there is no penalty that would have been otherwise incurred to enforce such minima and we have

$$\tilde{P}_{\mathrm{c}}(0) = 1. \tag{49}$$

Due to the oscillatory shape of $J_1(x), \tilde{P}_{\mathrm{c}}(\phi_\bullet)$ has an infinite number of sidelobe minima and peaks. Let $\tilde{\phi}_{\mathrm{n,c}}^{(n)}, \tilde{\phi}_{\mathrm{p,c}}^{(n)}$, and $\nu^{(n)}$ denote the $n$th sidelobe minimum point of $\tilde{P}_{\mathrm{c}}(\phi_\bullet)$, the $n$th sidelobe peak point of $\tilde{P}_{\mathrm{c}}(\phi_\bullet)$, and the $n$th positive root of $J_1(x)$, respectively. From (48) we have

$$\alpha\left(\tilde{\phi}_{\mathrm{n,c}}^{(n)}\right) = \nu^{(n)} \tag{50}$$

and, therefore,

$$\tilde{\phi}_{\mathrm{n,c}}^{(n)} = 2 \arcsin\left(\frac{\nu^{(n)}}{4\pi\tilde{R}}\right). \tag{51}$$

Taking the derivative with respect to $\phi_\bullet$ from (48) and equating the result to zero, it can be shown that $\alpha(\tilde{\phi}_{\mathrm{p,c}}^{(n)}) = \omega^{(n)}$ where $\omega^{(n)}$ is the $n$th positive solution to

$$xJ_0(x) = 2J_1(x). \tag{52}$$

As (52) is a univariate equation of $x, \alpha(\tilde{\phi}_{\mathrm{p,c}}^{(n)})$ is independent of $\tilde{R}$. Note also from (48) that, for any given $K, \tilde{P}_{\mathrm{c}}(\phi_\bullet)$ is a univariate function of $\alpha(\phi_\bullet)$. Therefore, $\tilde{P}_{\mathrm{c}}(\tilde{\phi}_{\mathrm{p,c}}^{(n)})$, the $n$th sidelobe peak of $\tilde{P}_{\mathrm{c}}(\phi_\bullet)$, is also fixed and cannot be adjusted by changing $\tilde{R}$. It should be stressed that $\tilde{\phi}_{\mathrm{p,c}}^{(n)}$ depends on $\tilde{R}$ as

$$\tilde{\phi}_{\mathrm{p,c}}^{(n)} = 2\arcsin\left(\frac{\omega^{(n)}}{4\pi\tilde{R}}\right). \tag{53}$$

Simple approximations of $\tilde{\phi}_{\mathrm{n,c}}^{(n)}$ and $\tilde{\phi}_{\mathrm{p,c}}^{(n)}$ can be obtained if one uses

$$J_1(x) \approx \sqrt{\frac{2}{\pi x}}\cos\left(x - \frac{3\pi}{4}\right) \qquad x \gg 1 \tag{54}$$

in (48) and simplifies the average beampattern expression to [1]

$$\tilde{P}_{\mathrm{c}}(\phi_\bullet) \approx \frac{1}{K} + \left(1 - \frac{1}{K}\right)\frac{8}{\pi\alpha(\phi_\bullet)^3}\cos^2\left(\alpha(\phi_\bullet) - \frac{3\pi}{4}\right) \tag{55}$$

for $\alpha(\phi_\bullet) \gg 1$. It can be shown from (55) that if $\tilde{R}$ is large enough such that $\alpha(\phi_\bullet) \triangleq 4\pi\tilde{R}\sin(\phi_\bullet/2) \gg 1$, then [1]

$$\tilde{\phi}_{\mathrm{n,c}}^{(n)} \approx 2\arcsin\left(\frac{n+1/4}{4\tilde{R}}\right), \tag{56}$$

$$\tilde{\phi}_{\mathrm{p,c}}^{(n)} \approx 2\arcsin\left(\frac{n+3/4}{4\tilde{R}}\right). \tag{57}$$

It also follows from (55) and (57) that [1]

$$\tilde{P}_{\mathrm{c}}\left(\tilde{\phi}_{\mathrm{p,c}}^{(n)}\right) \approx \frac{1}{K} + \left(1 - \frac{1}{K}\right)\cdot\frac{1}{\pi}\left(\frac{2}{\pi(n+3/4)}\right)^3. \tag{58}$$

Note from (58) that $\tilde{P}_{\mathrm{c}}(\tilde{\phi}_{\mathrm{p,c}}^{(1)})$ is the largest sidelobe peak and $\tilde{P}_{\mathrm{c}}(\tilde{\phi}_{\mathrm{p,c}}^{(n)})$ is almost proportional to $1/n^3$.

### *E. Average Beampattern When $\phi_l = \tilde{\phi}_{\mathrm{n,c}}^{(n)}$*

When the direction of each unintended receiver coincides with one of the minimum points of $\tilde{P}_{\mathrm{c}}(\phi_\bullet)$, that is,

$$\{\phi_1, \ldots, \phi_L\} \subseteq \left\{\tilde{\phi}_{\mathrm{n,c}}^{(1)}, \tilde{\phi}_{\mathrm{n,c}}^{(2)}, \ldots\right\} \tag{59}$$

we have that $J_1(\alpha(\phi_l)) = 0, l = 1, \ldots, L$, and, consequently, $\bar{\mathbf{g}}_0 = \mathbf{0}$. Using the latter result in (35), it follows that

$$\tilde{P}(\phi_\bullet) = \tilde{P}_{\mathrm{c}}(\phi_\bullet). \tag{60}$$

Equation (60) verifies that in the special case where (59) holds, the average beampattern of the proposed collaborative null-steering beamformer and that of the collaborative conventional beamformer are identical throughout the whole range of $\phi_\bullet$.

### *F. Approximate Average Beampattern for $\alpha(\phi_l) \gg 1$*

Note from (27) that as $\alpha(\phi_l)$ increases, $[\bar{\mathbf{g}}_0]_l$ converges to zero. In particular, when the angular distances between the AP and the unintended receivers are not very small and $\tilde{R}$ is large enough such that

$$\alpha(\phi_l) = 4\pi\tilde{R}\sin\left(\frac{\phi_l}{2}\right) \gg 1 \quad l = 1, \ldots, L \tag{61}$$

then (54) can be used in (27) to obtain

$$[\bar{\mathbf{g}}_0]_l \approx \frac{1}{\sqrt{\pi}}\cdot\left(\frac{2}{\alpha(\phi_l)}\right)^{\frac{3}{2}}\cos\left(\alpha(\phi_l) - \frac{3\pi}{4}\right) \tag{62}$$

for $l = 1, \ldots, L$. As such, when (61) holds, we have that $\bar{\mathbf{g}}_0^T\bar{\mathbf{E}}^{-1}\bar{\mathbf{g}}_0 \ll 1$. Using the latter inequality in (35), it follows that

$$\tilde{P}(\phi_\bullet) \approx \frac{1}{K} + \left(1 - \frac{1}{K}\right) \cdot\left(\frac{2}{\alpha(\phi_\bullet)}J_1\left(\alpha(\phi_\bullet)\right) - \bar{\mathbf{g}}_0^T\bar{\mathbf{E}}^{-1}\bar{\mathbf{g}}_{\phi_\bullet}\right)^2. \tag{63}$$

A direct result of (63) is that

$$\tilde{P}(0) \approx \frac{1}{K} + \left(1 - \frac{1}{K}\right)\left(1 - \bar{\mathbf{g}}_0^T\bar{\mathbf{E}}^{-1}\bar{\mathbf{g}}_0\right)^2 \approx 1. \tag{64}$$

Approximation (64) shows that if (61) holds, then $\tilde{P}(0)$ approaches its maximal value. In such a case, suppressing the power in the directions of the unintended receivers does not inflict a noticeable decrease in the received power at the AP.

Approximation (63) can be further simplified for those angles $\phi_\bullet$ that are not in a close proximity of any $\phi_l, l = 1, \ldots, L$. In fact, if $|\phi_\bullet - \phi_1|, \ldots, |\phi_\bullet - \phi_L|$ are large enough such that

$$|\alpha(\phi_\bullet - \phi_l)| = 4\pi\tilde{R}\sin\left(\frac{|\phi_\bullet - \phi_l|}{2}\right) \gg 1 \qquad l = 1, \ldots, L, \tag{65}$$

then

$$[\bar{\mathbf{g}}_{\phi_\bullet}]_l \approx \frac{1}{\sqrt{\pi}}\cdot\left(\frac{2}{|\alpha(\phi_\bullet - \phi_l)|}\right)^{\frac{3}{2}} \times\cos\left(|\alpha(\phi_\bullet - \phi_l)| - \frac{3\pi}{4}\right) \tag{66}$$

for $l = 1, \ldots, L$. In such a case, it follows from (62) and (66) that $|\bar{\mathbf{g}}_0^T\bar{\mathbf{E}}^{-1}\bar{\mathbf{g}}_{\phi_\bullet}| \ll |2J_1(\alpha(\phi_\bullet))/\alpha(\phi_\bullet)|$ and

$$\tilde{P}(\phi_\bullet) \approx \frac{1}{K} + \left(1 - \frac{1}{K}\right)\left(\frac{2}{\alpha(\phi_\bullet)}J_1(\alpha(\phi_\bullet))\right)^2 = \tilde{P}_{\mathrm{c}}(\phi_\bullet). \tag{67}$$

Equation (67) states that if (61) holds and $\phi_\bullet$ is not close to the direction of any of the unintended receivers, then $P(\phi_\bullet)$ is approximately equal to the average gain of the collaborative conventional beamformer.

The discussion of this subsection can be summarized as follows: Assume that (61) holds. Then, $\tilde{P}(\phi_\bullet)$ looks similar to $\tilde{P}_{\rm c}(\phi_\bullet)$ for all $\phi_\bullet$ far enough from any $\phi_1,\ldots,\phi_L$. In particular, $\tilde{P}(\phi_\bullet)$ and $\tilde{P}_{\rm c}(\phi_\bullet)$ have similar sets of minimum and peak points in the angular intervals that are not close to any $\phi_1,\ldots,\phi_L$. Note that $\tilde{P}(\phi_\bullet)$ has additional minima at $\phi_1,\ldots,\phi_L$ and when $\phi_\bullet$ is close to a $\phi_l$, (63) (and not (67)) is a reliable approximation of $\tilde{P}(\phi_\bullet)$.

Before closing this section, it should be mentioned that if the number of collaborating nodes $K$ is small, then there can be a noticeable discrepancy between the average beampattern $\tilde{P}(\phi_\bullet)$ and any particular realization of the beampattern $P(\phi_\bullet|\mathbf{z})$. In such cases, an analysis regarding the statistical properties of the beampattern is useful. Using the same steps as in ([1], Section IV) to carry out such an analysis, it can be shown that the statistical properties of $P(\phi_\bullet|\mathbf{z})$ and that of the beampattern of the conventional beamformer [1] are quite similar. In particular, if (61) holds, then the complementary cumulative distribution function of the gain of the proposed beamformer at any arbitrary $\phi_\bullet$ is approximately equal to [1, Eq. (47)].

## V. Sidelobe Peak Reduction

In many practical scenarios, the directions of unintended receivers are unknown. In such cases, it may be more beneficial to form a transmit beam with small sidelobe peaks to avoid the signal impinging on the unintended receivers with a strong power. As shown in Section IV-D (see also [1]), it is not possible to decrease the sidelobe peaks of the collaborative conventional beamformer. This is an undesired property as, for instance, $\tilde{P}_{\rm c}(\tilde{\phi}_{\rm p,c}^{(1)})$, the most prominent sidelobe peak of $\tilde{P}_{\rm c}(\phi_\bullet)$, may be unacceptably large. In contrast to the collaborative conventional beamformer, the sidelobe peaks of the proposed collaborative null-steering beamformer are not fixed and depend on the locations of the devised minima $\phi_1,\ldots,\phi_L$. Therefore, positioning $\phi_1,\ldots,\phi_L$ at proper locations, or, equivalently, assuming virtual unintended receivers at proper directions, $\bar{\mathbf{w}}_{\rm ns}$ may alternatively be used to decrease the sidelobe peaks.

Let $\tilde{P}(\phi_\bullet,\phi_1)$ denote the average beampattern of a collaborative null-steering beamformer with a single devised minimum at $\phi_1$. Note that the second argument is added to $\tilde{P}(\phi_\bullet,\phi_1)$ to stress the fact that $\phi_1$ is a design parameter. Let us also denote $\mathcal{A}\subseteq(0,\pi)$ such that

$$\tilde{P}(0,\phi_1)\geq 0.95\quad \forall\phi_1\in\mathcal{A}. \tag{68}$$

As follows from (68), selecting $\phi_1$ from $\mathcal{A}$ guarantees that there may be only a negligible decrease in the received power at the AP due to the use of $\bar{\mathbf{w}}_{\rm ns}$ to enforce a devised minimum. In what follows, we aim to find $\check{\phi}_1$ such that: 1) $\check{\phi}_1\in\mathcal{A}$; and 2) Among all $\phi_1\in\mathcal{A}$, $\check{\phi}_1$ minimizes the largest sidelobe peak of $\tilde{P}(\phi_\bullet,\phi_1)$.

When $L=1$, we have $\bar{\mathbf{g}}_{\phi_\bullet}=2J_1(\alpha(\phi_\bullet-\phi_1))/\alpha(\phi_\bullet-\phi_1)$ for $\phi_\bullet\neq\phi_1$ and $\bar{\mathbf{E}}=1$. Therefore, for $\phi_\bullet\neq\phi_1$, the average beampattern expression (35) reduces to

$$\tilde{P}(\phi_\bullet,\phi_1)=\frac{1}{K}+\left(1-\frac{1}{K}\right)\cdot\frac{1}{1-\left(\frac{2J_1(\alpha(\phi_1))}{\alpha(\phi_1)}\right)^2}\cdot\left(\frac{2J_1(\alpha(\phi_\bullet))}{\alpha(\phi_\bullet)}-\frac{2J_1(\alpha(\phi_1))}{\alpha(\phi_1)}\cdot\frac{2J_1(\alpha(\phi_\bullet-\phi_1))}{\alpha(\phi_\bullet-\phi_1)}\right)^2 \tag{69}$$

and, hence,

$$\begin{aligned}\tilde{P}(0,\phi_1)&=1-\left(\frac{2J_1(\alpha(\phi_1))}{\alpha(\phi_1)}\right)^2+\frac{1}{K}\left(\frac{2J_1(\alpha(\phi_1))}{\alpha(\phi_1)}\right)^2\\&\geq 1-\left(\frac{2J_1(\alpha(\phi_1))}{\alpha(\phi_1)}\right)^2.\end{aligned} \tag{70}$$

It is direct to show from (70) that

$$\mathcal{A}=\left[2\arcsin\left(\frac{3.01}{4\pi\tilde{R}}\right),\pi\right) \tag{71}$$

satisfies (68). Note from (71) that $\alpha(\check{\phi}_1)\geq 3.01$ and, further, for any $\phi_1\in\mathcal{A}$ we have

$$\tilde{P}(\phi_\bullet,\phi_1)\approx\frac{1}{K}+\left(1-\frac{1}{K}\right)\left(\frac{2J_1\left(\alpha(\phi_\bullet)\right)}{\alpha(\phi_\bullet)}-\frac{2J_1(\alpha(\phi_1))}{\alpha(\phi_1)}\cdot\frac{2J_1(\alpha(\phi_\bullet-\phi_1))}{\alpha(\phi_\bullet-\phi_1)}\right)^2. \tag{72}$$

Let $\tilde{\phi}_{\rm p}^{(\star)}(\phi_1)$ denote the largest sidelobe peak point of $\tilde{P}(\phi_\bullet,\phi_1)$ for a given $\phi_1$. The argument $\phi_1$ is used in $\tilde{\phi}_{\rm p}^{(\star)}(\phi_1)$ to emphasize the fact that the largest sidelobe peak point of the average beampattern depends on $\phi_1$. Moreover, note that, in contrast to the collaborative conventional beamformer, there is no guarantee that the first sidelobe peak of $\tilde{P}(\phi_\bullet,\phi_1)$ is its largest one. Therefore, the superscript $^{(\star)}$ (and not $^{(1)}$) is used to denote the index of the largest sidelobe peak of $\tilde{P}(\phi_\bullet,\phi_1)$.

As will be shown later, it is also useful to obtain reasonable upper bounds on both $\alpha(\check{\phi}_1)$ and $\alpha(\tilde{\phi}_{\rm p}^{(\star)}(\phi_1))$ as follows:

*Upper Bound on $\alpha(\check{\phi}_1)$:* We have from (50) that $\alpha(\tilde{\phi}_{\rm n,c}^{(1)})=\nu^{(1)}=3.8317$ and $\alpha(\tilde{\phi}_{\rm n,c}^{(2)})=\nu^{(2)}=7.0156$ and, therefore, $3.8317<\alpha(\tilde{\phi}_{\rm p,c}^{(1)})<7.0156$. If $\alpha(\check{\phi}_1)$ is excessively large, say, $\alpha(\check{\phi}_1)\geq\nu^{(3)}=10.1735$, then $\alpha(\check{\phi}_1-\tilde{\phi}_{\rm p,c}^{(1)})\gg 1$, and, hence, according to (65) and (67), $\tilde{P}(\tilde{\phi}_{\rm p,c}^{(1)},\check{\phi}_1)\approx\tilde{P}_{\rm c}(\tilde{\phi}_{\rm p,c}^{(1)})$. The latter result indicates that the average gain of the collaborative null-steering beamformer at $\tilde{\phi}_{\rm p,c}^{(1)}$ is approximately equal to the largest sidelobe peak of $\tilde{P}_{\rm c}(\phi_\bullet)$. This defies the purpose of using the collaborative null-steering beamformer to reduce the largest sidelobe peak. As such, we assume that $\alpha(\check{\phi}_1)\leq\nu^{(3)}$. We will verify later that $\alpha(\check{\phi}_1)$ is considerably less than $\nu^{(3)}$.

*Upper Bound on $\alpha(\tilde{\phi}_{\rm p}^{(\star)}(\phi_1))$:* Approximation (54) shows that as $\alpha(\phi_\bullet)$ increases, $2J_1(\alpha(\phi_\bullet))/\alpha(\phi_\bullet)$ converges to zero with the rate $\mathcal{O}(\alpha(\phi_\bullet)^{3/2})$. Taking into account this fact, it can be observed from (72) that, irrespective to $\phi_1,\alpha(\tilde{\phi}_{\rm p}^{(\star)}(\phi_1))$ cannot be very large. In what follows, we assume that $0<\alpha(\tilde{\phi}_{\rm p}^{(\star)}(\phi_1))\leq\nu^{(3)}$. Our developments will later show that the above upper bound is in fact loose.

Let us now turn our attention back to $\tilde{P}(\phi_\bullet,\phi_1)$ in (72). The RHS of (72) depends on $\alpha(\phi_1),\alpha(\phi_\bullet)$, and $\alpha(\phi_\bullet-\phi_1)$. Note that

$$\begin{aligned}\alpha(\phi_\bullet-\phi_1)&=4\pi\tilde{R}\sin\left(\frac{\phi_\bullet-\phi_1}{2}\right)\\&=\alpha(\phi_\bullet)\cos\left(\frac{\phi_1}{2}\right)-\alpha(\phi_1)\cos\left(\frac{\phi_\bullet}{2}\right)\end{aligned}$$

$$= \alpha(\phi_\bullet)\sqrt{1-\left(\frac{\alpha(\phi_1)}{4\pi\tilde{R}}\right)^2} - \alpha(\phi_1)\sqrt{1-\left(\frac{\alpha(\phi_\bullet)}{4\pi\tilde{R}}\right)^2}. \quad (73)$$

Using (73) in (72), it immediately follows that, in general, $\tilde{P}(\phi_\bullet,\phi_1)$ is a function of $\alpha(\phi_1),\alpha(\phi_\bullet)$, and $\tilde{R}$. However, the so-obtained bounds on $\alpha(\check{\phi}_1)$ and $\alpha(\tilde{\phi}_{\rm p}^{(\star)}(\phi_1))$ suggest that, to find $\check{\phi}_1$ and $\tilde{\phi}_{\rm p}^{(\star)}(\phi_1)$, it is only required to search in the intervals corresponding to $\alpha(\phi_1)\in[3.01,\nu^{(3)}]$ and $\alpha(\phi_\bullet)\in(0,\nu^{(3)}]$, respectively. If $\tilde{R}\geq 5$, we have in the latter intervals that

$$\min\left\{\sqrt{1-\left(\frac{\alpha(\phi_1)}{4\pi\tilde{R}}\right)^2},\sqrt{1-\left(\frac{\alpha(\phi_\bullet)}{4\pi\tilde{R}}\right)^2}\right\}=0.9868. \quad (74)$$

Using (74) in (73), it holds for any $\tilde{R}\geq 5,\alpha(\phi_1)\in[3.01,\nu^{(3)}]$, and $\alpha(\phi_\bullet)\in(0,\nu^{(3)}]$ that

$$\alpha(\phi_\bullet-\phi_1)\approx\alpha(\phi_\bullet)-\alpha(\phi_1). \quad (75)$$

Approximation (75) shows that if $\tilde{R}\geq 5$ and $\alpha(\phi_1)$ and $\alpha(\phi_\bullet)$ are in the intervals of our concern, then $\tilde{P}(\phi_\bullet,\phi_1)$ is solely a function of two variables $\alpha(\phi_1)$ and $\alpha(\phi_\bullet)$ and can be equivalently represented as

$$\tilde{P}(\alpha(\phi_\bullet),\alpha(\phi_1))\approx\frac{1}{K}+\left(1-\frac{1}{K}\right)\left(\frac{2J_1(\alpha(\phi_\bullet))}{\alpha(\phi_\bullet)} - \frac{2J_1(\alpha(\phi_1))}{\alpha(\phi_1)}\cdot\frac{2J_1(\alpha(\phi_\bullet)-\alpha(\phi_1))}{\alpha(\phi_\bullet)-\alpha(\phi_1)}\right)^2. \quad (76)$$

Approximation (76) not only represents the average beampattern expression as an explicit function of $\alpha(\phi_1)$ and $\alpha(\phi_\bullet)$, but also implies that, if $\tilde{R}\geq 5$, then $\alpha(\tilde{\phi}_{\rm p}^{(\star)}(\phi_1))$ and $\alpha(\check{\phi}_1)$ are independent of $\tilde{R}$. The latter result is of considerable practical importance, as it shows that if $\tilde{R}\geq 5$, then $\alpha(\check{\phi}_1)$ is globally optimal for any WSN cluster size.

Using (76) and the following two-step procedure, $\alpha(\check{\phi}_1)$ can be directly determined:

1) For every $\alpha(\phi_1)\in[3.01,\nu^{(3)}]$, obtain $\alpha(\tilde{\phi}_{\rm p}^{(\star)}(\phi_1))$ as the root of
$$\frac{\partial\tilde{P}(\alpha(\phi_\bullet),\alpha(\phi_1))}{\partial\alpha(\phi_1)}=0 \quad (77)$$
that corresponds to the largest local maximum of $\tilde{P}(\alpha(\phi_\bullet),\alpha(\phi_1))$ in the interval $\alpha(\phi_\bullet)\in(0,\nu^{(3)}]$.
2) Obtain
$$\alpha(\check{\phi}_1)=\arg\min\tilde{P}\left(\alpha\left(\tilde{\phi}_{\rm p}^{(\star)}(\phi_1)\right),\alpha(\phi_1)\right) \quad (78)$$
for $\alpha(\phi_1)\in[3.01,\nu^{(3)}]$.

Note from (76) that all roots of (77) including $\alpha(\tilde{\phi}_{\rm p}^{(\star)}(\phi_1))$ are independent from $K$. It is also straightforward to observe from (76) and (78) that $\alpha(\check{\phi}_1)$ is independent from $K$.

Fig. 2 displays $\tilde{P}(\alpha(\tilde{\phi}_{\rm p}^{(\star)}(\phi_1)),\alpha(\phi_1))$ (dB) versus $\alpha(\phi_1)\in[3.01,\nu^{(3)}]$ for $K\to\infty$. For the sake of comparison, $\tilde{P}_{\rm c}(\tilde{\phi}_{{\rm p},c}^{(1)})$ is also shown with a dash-dotted line. It should also be mentioned that the part of the curve of $\tilde{P}(\alpha(\tilde{\phi}_{\rm p}^{(\star)}(\phi_1)),\alpha(\phi_1))$ that is plotted with a bold line corresponds to those values of $\alpha(\phi_1)$ for which $\tilde{\phi}_{\rm p}^{(\star)}(\phi_1)=\tilde{\phi}_{\rm p}^{(2)}(\phi_1)$. We have $\tilde{\phi}_{\rm p}^{(\star)}(\phi_1)=\tilde{\phi}_{\rm p}^{(1)}(\phi_1)$ in other parts of the curve.

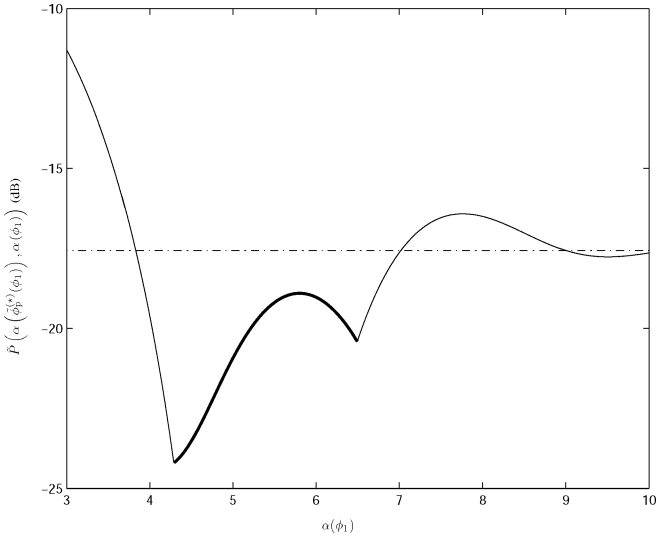


Fig. 2. $\tilde{P}(\alpha(\tilde{\phi}_{\rm p}^{(\star)}(\phi_1)),\alpha(\phi_1))$ (dB) versus $\alpha(\phi_1)\in[3.01,\nu^{(3)}]$ for $K\to\infty$.

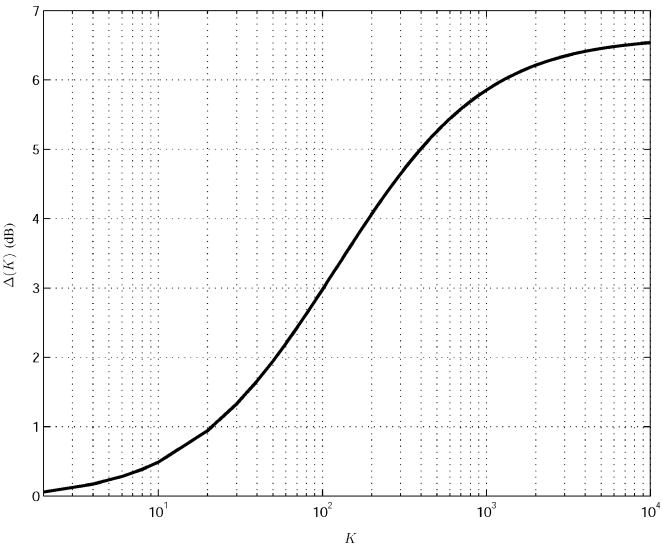


Fig. 3. $\Delta(K)$ (dB) versus $K$.

It can be observed from Fig. 2 that $\alpha(\check{\phi}_1)=4.2950$. Note that if $\alpha(\check{\phi}_1)$ is selected, then the first and the second sidelobe peaks of the average beampattern are equal to each other but are larger than all other sidelobe peaks and we have $\alpha(\tilde{\phi}_{\rm p}^{(1)}(\check{\phi}_1))=5.2776$ and $\alpha(\tilde{\phi}_{\rm p}^{(2)}(\check{\phi}_1))=8.1822$. Although $\alpha(\check{\phi}_1)$ and $\alpha(\tilde{\phi}_{\rm p}^{(\star)}(\check{\phi}_1))$ are independent from $K$, it follows from (76) that

$$\Delta(K)\triangleq 10\log_{10}\left(\frac{\tilde{P}_{\rm c}\left(\tilde{\phi}_{{\rm p},c}^{(1)}\right)}{\tilde{P}\left(\alpha\left(\tilde{\phi}_{\rm p}^{(\star)}(\check{\phi}_1)\right),\alpha(\check{\phi}_1)\right)}\right) \quad (79)$$

is a function of $K$. Note that $\Delta(K)$ is the decrease in the largest sidelobe peak of the average beampattern if the collaborative null-steering beamformer with a single devised minimum at $\check{\phi}_1$

is used in lieu of the collaborative conventional beamformer. Fig. 3 displays $\Delta(K)$ (dB) versus $K$. As can be observed from Fig. 3, $\Delta(K)$ is a positive and increasing function of $K$. As such, irrespective to $K$, the maximum sidelobe peak of $\tilde{P}(\phi_\bullet, \check{\phi}_1)$ is always smaller than that of $\tilde{P}_{\rm c}(\phi_\bullet)$. Moreover, as $K$ increases, the gap between the maximum sidelobe peaks of $\tilde{P}(\phi_\bullet, \check{\phi}_1)$ and $\tilde{P}_{\rm c}(\phi_\bullet)$ grows. Note from Fig. 3 that $\Delta(100) \approx 3$ (dB) and as $K \to \infty, \Delta(K)$ increases up to 6.6 (dB).

Our results in this section can be summarized as follows:

- Assume that $\tilde{R} \geq 5$ and $\bar{\mathbf{w}}_{\rm ns}$ with $L = 1$ is used to form a transmission beam towards the AP. Then, among all locations of the devised minimum $\phi_1$ that have negligible impact on the received power at the AP, the optimal location that additionally minimizes the largest sidelobe peak of $\tilde{P}(\phi_\bullet, \phi_1)$ is given by

$$\check{\phi}_1 \approx 2 \arcsin\left(\frac{4.2950}{4\pi\tilde{R}}\right). \tag{80}$$

  Positioning a minimum at $\check{\phi}_1$, the first and the second sidelobe peaks become equal and we have

$$\begin{aligned} \tilde{\phi}_{\rm p}^{(\star)}(\phi_1) = \tilde{\phi}_{\rm p}^{(1)}(\phi_1) &\approx 2 \arcsin\left(\frac{5.2776}{4\pi\tilde{R}}\right) \\ \tilde{\phi}_{\rm p}^{(\star)}(\phi_1) = \tilde{\phi}_{\rm p}^{(2)}(\phi_1) &\approx 2 \arcsin\left(\frac{8.1758}{4\pi\tilde{R}}\right). \end{aligned} \tag{81}$$

  Moreover, if $\check{\phi}_1$ is used, then, depending on $K$, the resulting largest sidelobe peaks can be up to 6.6 (dB) less than the largest sidelobe peak of the collaborative conventional beamformer.

## VI. Simulations

Simulations are conducted to validate the analytical results of Sections IV and V. In all examples $\tilde{R} = 10$ is selected. Fig. 4 displays $\tilde{P}(\phi_\bullet)$ versus $\phi_\bullet$ for $K = 20$ and three different sets of devised minima. The dotted, the dashed, and the continuous curves in Fig. 4 show $\tilde{P}(\phi_\bullet)$ versus $\phi_\bullet$ for $L = 1$ with $\boldsymbol{\phi}_1 = [\phi_1] = [4.3]$ (deg), for $L = 2$ with $\boldsymbol{\phi}_2 = [\phi_1, \phi_2] = [4.3, 6.2]$ (deg), and for $L = 3$ with $\boldsymbol{\phi}_3 = [\phi_1, \phi_2, \phi_3] = [4.3, 6.2, 9.5]$ (deg), respectively. For the sake of comparison, $\tilde{P}_{\rm c}(\phi_\bullet)$ is also plotted versus $\phi_\bullet$ in this figure. It can be verified from Fig. 4 that each $\tilde{P}(\phi_\bullet)$ curve has minima at the angles given by the entries of its associated $\boldsymbol{\phi}_l$. Moreover, as (61) holds for all devised minima, we have that $\tilde{P}(0) \approx 1$ in all cases. This corroborates our discussion in Section IV-F.

Similar sets of curves as in Fig. 4 are displayed for $K = 200$ and $K \to \infty$ in Figs. 5 and 6, respectively. It can be observed from Figs. 4–6 that as $K$ increases, the minima of the $\tilde{P}(\phi_\bullet)$ curves decrease. In particular, when $K \to \infty$, each $\tilde{P}(\phi_\bullet)$ curve has zeros (deep nulls) at the angles specified by the entries of its associated $\boldsymbol{\phi}_l$. This further verifies our discussion at the end of Section IV-B. Note that all curves also have additional minima at angles other than those specified by $\boldsymbol{\phi}_l$. As discussed in Sections IV-D and IV-F this is due to the oscillatory nature of the Bessel function.

Fig. 7 plots $\tilde{P}(\phi_\bullet)$ versus $\phi_\bullet$ for $K = 200$ and two different sets of devised minima at $[\phi_1, \phi_2] = [5, 9]$ (deg) and $[\phi_1, \phi_2] = [2.5, 9]$ (deg). The curve of $\tilde{P}_{\rm c}(\phi_\bullet)$ versus $\phi_\bullet$ is also displayed in this figure. Fig. 7 shows that all devised minima are enforced at the intended locations. Note that if $[\phi_1, \phi_2] = [5, 9]$ (deg), then (61) holds. Therefore, $\tilde{P}(0) \approx 1$ and, moreover, increasing $\phi_\bullet - \phi_2, \tilde{P}(\phi_\bullet)$ tends to approach $\tilde{P}_{\rm c}(\phi_\bullet)$. This further supports our discussion in Section IV-F. In contrast to the case where $[\phi_1, \phi_2] = [5, 9]$ (deg), (61) does not hold when $[\phi_1, \phi_2] = [2.5, 9]$ (deg). Fig. 7 shows that $\tilde{P}(0)$ noticeably decreases in the latter case.

Fig. 8 shows $\tilde{P}(\phi_\bullet, \check{\phi}_1)$ and $\tilde{P}_{\rm c}(\phi_\bullet)$ versus $\alpha(\phi_\bullet)$ for $K = 200$. As can be observed from Fig. 8, the first and the second sidelobe peaks of $\tilde{P}(\phi_\bullet, \check{\phi}_1)$ are equal and both are much smaller than the first sidelobe peak of $\tilde{P}_{\rm c}(\phi_\bullet)$. This validates the analytical results of Section V and confirms the effectiveness of selecting $\check{\phi}_1$ as in (80) to reduce the sidelobe peaks of the average beampattern.

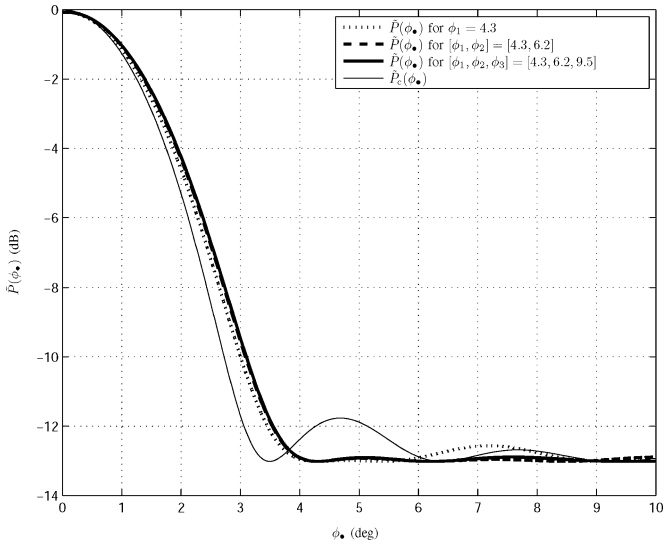


Fig. 4. $\tilde{P}(\phi_\bullet)$ (dB) versus $\phi_\bullet$ (deg) for $K = 20$ and three different sets of devised minima.

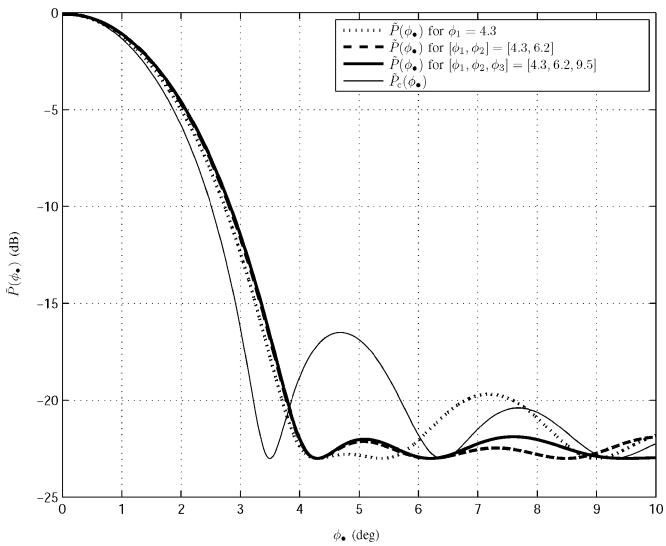


Fig. 5. $\tilde{P}(\phi_\bullet)$ (dB) versus $\phi_\bullet$ (deg) for $K = 200$ and three different sets of devised minima.

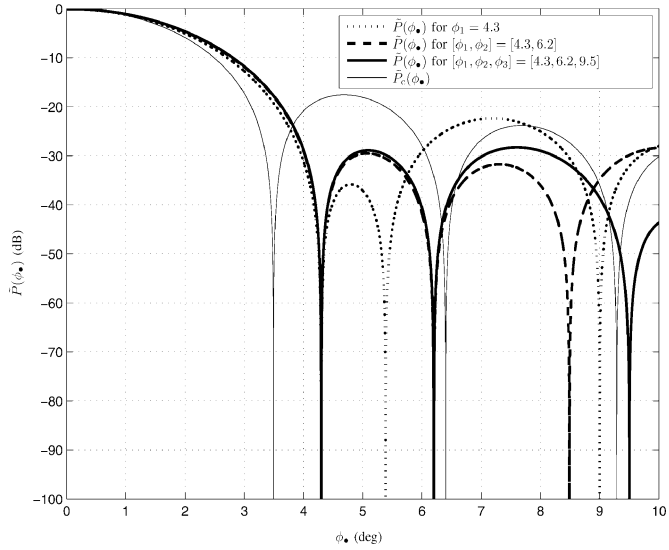


Fig. 6. $\bar{P}(\phi_\bullet)$ (dB) versus $\phi_\bullet$ (deg) for $K \to \infty$ and three different sets of devised minima.

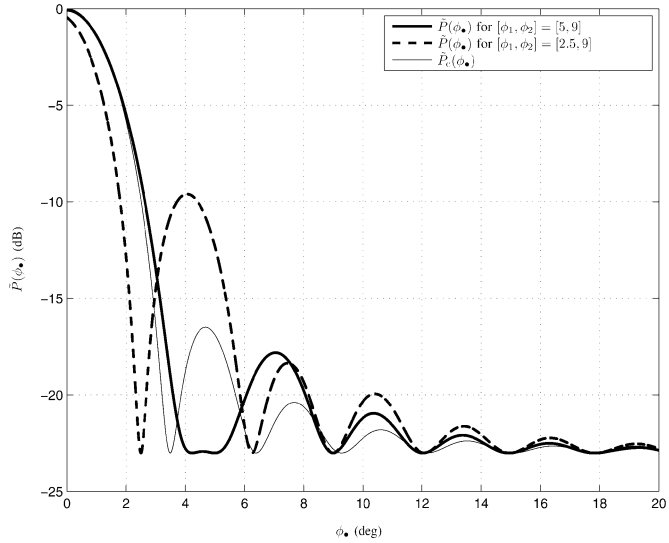


Fig. 7. $\bar{P}(\phi_\bullet)$ (dB) versus $\phi_\bullet$ (deg) for $K = 200$ and two sets of $[\phi_1, \phi_2] = [5, 9]$ (deg) and $[\phi_1, \phi_2] = [2.5, 9]$ (deg).

## VII. Conclusion

A collaborative null-steering beamformer has been proposed for uniformly distributed WSNs that forms the transmit beam towards the intended AP while substantially attenuating the transmit power in the directions of the unintended receivers. In contrast to its existing counterparts in the array processing literature, the proposed beamformer complies with the distributed nature of WSNs and can be implemented in the networks wherein each node is unaware of the locations of all other nodes. The average beampattern expression of the proposed collaborative null-steering beamformer has been derived and its properties have been analytically studied. It has been proven that the average gain of the proposed beamformer is inversely proportional to the number of nodes in the directions of unintended receivers. When the angular distances between the AP and the unintended receivers are not very small and the collaborating nodes are distributed on a disc with a large-enough radius, it has been further shown that the gain of the proposed beamformer is approximately equal to that of the collaborative conventional beamformer in directions with far angular distance from any unintended receiver.

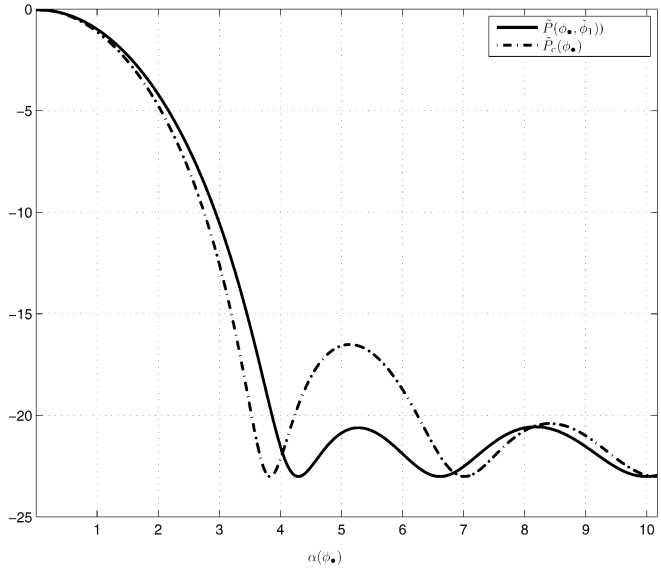


Fig. 8. $P(\phi_\bullet, \check{\phi}_1)$ (dB) and $\bar{P}_c(\phi_\bullet)$ (dB) versus $\alpha(\phi_\bullet)$ and $K = 200$.

It has been demonstrated that the proposed collaborative null-steering beamformer can be used in lieu of the collaborative conventional beamformer to avoid average beampatterns with excessively large sidelobe peaks. To this end, a collaborative null-steering beamformer has been designed that positions a single minimum point at the optimal direction such that the resulting average beampattern has the smallest possible largest sidelobe peak and, at the same time, the gain of the beamformer does not noticeably decrease in the direction of the AP.

## Appendix A
## Proof of Theorem 1

As $\mathbf{a}_{\phi_m}^H \mathbf{a}_{\phi_m} = K$, it is straightforward to show that (21), (24), and (25) are correct for $m = n$. The proof of (21) and (23) for $m \neq n$ is similar to the discussion prior to [1, Eq. (10)]. First, note from (7) that

$$\begin{aligned}\frac{1}{K}\mathbf{a}_{\phi_m}^H \mathbf{a}_{\phi_n} &= \frac{1}{K}\sum_{k=1}^{K} e^{j\frac{2\pi}{\lambda} r_k(\cos(\phi_n - \psi_k) - \cos(\phi_m - \psi_k))} \\ &= \frac{1}{K}\sum_{k=1}^{K} e^{j4\pi\tilde{R}\sin(\frac{\phi_n - \phi_m}{2})\tilde{r}_k \sin\tilde{\psi}_k} \\ &= \frac{1}{K}\sum_{k=1}^{K} e^{j\alpha(\phi_n - \phi_m)z_k} \end{aligned} \tag{82}$$

where $\tilde{r}_k \triangleq r_k/R, \tilde{\psi}_k \triangleq \psi_k - ((\phi_n + \phi_m)/2)$, and $z_k$ is given by (22) and can be equivalently represented as $z_k = \tilde{r}_k \sin\tilde{\psi}_k$. As all nodes are uniformly distributed on $D(O, R)$, it follows that $\tilde{r}_k, k = 1, \ldots, K$ are i.i.d. random variables with the following PDF:

$$f_{\tilde{r}_k}(r) = 2r \quad r \in [0, 1]. \tag{83}$$

Similarly, $\tilde{\psi}_k, k = 1, \ldots, K$ are also i.i.d. random variables and we have

$$f_{\tilde{\psi}_k}(\psi) = \frac{1}{2\pi}, \quad \psi \in [-\pi, \pi). \tag{84}$$

As $\tilde{r}_k$ and $\tilde{\psi}_k$ are i.i.d. random variables with the above PDFs, it is direct to show that [1] $z_1, \ldots, z_K$ are also i.i.d. random variables with the PDF given by (23). From (21) and the fact that $z_1, \ldots, z_K$ are identically distributed, we have

$$\frac{1}{K}\mathrm{E}\left\{\mathbf{a}_{\phi_m}^H \mathbf{a}_{\phi_n}\right\} = \mathrm{E}\left\{e^{j\alpha(\phi_n - \phi_m)z_k}\right\} \tag{85}$$

Moreover, it follows from (23) that

$$\begin{aligned}
&\mathrm{E}\left\{e^{j\alpha(\phi_n-\phi_m)z_k}\right\} \\
&= \frac{2}{\pi}\int_{-1}^{1} e^{j\alpha(\phi_n-\phi_m)z}\sqrt{1-z^2}dz \\
&= \frac{2}{\pi}\int_{0}^{\pi} \sin^2\theta e^{j\alpha(\phi_n-\phi_m)\cos\theta}d\theta \\
&= \frac{2}{j\pi\alpha(\phi_n-\phi_m)}\int_{0}^{\pi} e^{j\alpha(\phi_n-\phi_m)\cos\theta}\cos\theta d\theta \\
&= \frac{2}{\alpha(\phi_n-\phi_m)}J_1(\alpha(\phi_n-\phi_m))
\end{aligned} \tag{86}$$

where the second line is due to the change of variable $\cos\theta \triangleq z$, the third line is obtained using the integration by parts, and the last line is due to the fact that $J_1(x) = (1/j\pi)\int_0^\pi e^{jx\cos\theta}\cos\theta d\theta$.

Finally, as $z_k, k = 1, \ldots, K$ are i.i.d. and $\mathrm{E}\{e^{j\alpha(\phi_n-\phi_m)z_k}\}$ is bounded, the strong law of large numbers applies to (21) and yields (25). This completes the proof.

## Appendix B
## Proof of Theorem 2

It follows from (33) that

$$P(\phi_\bullet|\mathbf{z}) = \frac{\eta_1 - \eta_2 - \eta_2^* + \eta_3}{1 - \bar{\mathbf{g}}_0^T\bar{\mathbf{E}}^{-1}\bar{\mathbf{g}}_0} \tag{87}$$

where

$$\eta_1 \triangleq \frac{1}{K^2}\mathbf{a}_{\phi_\bullet}^H\mathbf{a}_0\mathbf{a}_0^H\mathbf{a}_{\phi_\bullet} \tag{88}$$

$$\eta_2 \triangleq \frac{1}{K^2}\mathbf{a}_{\phi_\bullet}^H\mathbf{A}\bar{\mathbf{E}}^{-1}\bar{\mathbf{g}}_0\mathbf{a}_0^H\mathbf{a}_{\phi_\bullet} \tag{89}$$

$$\eta_3 \triangleq \frac{1}{K^2}\mathbf{a}_{\phi_\bullet}^H\mathbf{A}\bar{\mathbf{E}}^{-1}\bar{\mathbf{g}}_0\bar{\mathbf{g}}_0^T\bar{\mathbf{E}}^{-1}\mathbf{A}^H\mathbf{a}_{\phi_\bullet} \tag{90}$$

Therefore, we have

$$\tilde{P}(\phi_\bullet) = \frac{\mathrm{E}_{\mathbf{z}}\{\eta_1\} - \mathrm{E}_{\mathbf{z}}\{\eta_2\} - \mathrm{E}_{\mathbf{z}}\{\eta_2^*\} + \mathrm{E}_{\mathbf{z}}\{\eta_3\}}{1 - \bar{\mathbf{g}}_0^T\bar{\mathbf{E}}^{-1}\bar{\mathbf{g}}_0}. \tag{91}$$

Using (21) in (88) yields

$$\begin{aligned}
\eta_1 &= \frac{1}{K^2}\sum_{k=1}^{K}\sum_{s=1}^{K} e^{j\alpha(\phi_\bullet)z_k}e^{-j\alpha(\phi_\bullet)z_s} \\
&= \frac{1}{K} + \frac{1}{K^2}\sum_{k=1}^{K} e^{j\alpha(\phi_\bullet)z_k}\sum_{\substack{s=1\\ s\neq k}}^{K} e^{-j\alpha(\phi_\bullet)z_s}.
\end{aligned} \tag{92}$$

Taking an expectation operation from both sides of (92) and using (24), it follows that

$$\mathrm{E}_{\mathbf{z}}\{\eta_1\} = \frac{1}{K} + \left(1 - \frac{1}{K}\right)\left(\frac{2J_1(\alpha(\phi_\bullet))}{\alpha(\phi_\bullet)}\right)^2. \tag{93}$$

It directly follows from the definition of $\mathbf{A}$ and (89) that

$$\eta_2 = \sum_{l=1}^{L}[\bar{\mathbf{E}}^{-1}\bar{\mathbf{g}}_0]_l\theta_l^{(1)} \tag{94}$$

where

$$\theta_l^{(1)} \triangleq \frac{1}{K^2}\mathbf{a}_{\phi_\bullet}^H\mathbf{a}_{\phi_l}\mathbf{a}_0^H\mathbf{a}_{\phi_\bullet}. \tag{95}$$

From (7) we have

$$\begin{aligned}
\theta_l^{(1)} &= \frac{1}{K^2}\sum_{k=1}^{K}\sum_{s=1}^{K} e^{j\frac{2\pi}{\lambda}r_k(\cos(\phi_l-\psi_k)-\cos(\phi_\bullet-\psi_k))} \\
&\quad \cdot e^{j\frac{2\pi}{\lambda}r_s(\cos(\phi_\bullet-\psi_s)-\cos(\psi_s))} \\
&= \frac{1}{K^2}\sum_{k=1}^{K} e^{j\frac{2\pi}{\lambda}r_k(\cos(\phi_l-\psi_k)-\cos(\psi_k))} \\
&\quad + \frac{1}{K^2}\left(\sum_{k=1}^{K} e^{j\frac{2\pi}{\lambda}r_k(\cos(\phi_l-\psi_k)-\cos(\phi_\bullet-\psi_k))}\right. \\
&\quad \left.\cdot\sum_{\substack{s=1\\ s\neq k}}^{K} e^{j\frac{2\pi}{\lambda}r_s(\cos(\phi_\bullet-\psi_s)-\cos(\psi_s))}\right) \\
&= \frac{1}{K^2}\sum_{k=1}^{K} e^{j\alpha(\phi_l)z_k} \\
&\quad + \frac{1}{K^2}\sum_{k=1}^{K} e^{j\alpha(\phi_l-\phi_\bullet)z_k}\sum_{\substack{s=1\\ s\neq k}}^{K} e^{j\alpha(\phi_\bullet)z_s}
\end{aligned} \tag{96}$$

where its last line is obtained following the same steps as in (82). Taking an expectation operation from both sides of (96) and using (24), we have

$$\begin{aligned}
\mathrm{E}_{\mathbf{z}}\left\{\theta_l^{(1)}\right\} &= \frac{1}{K}\cdot\frac{2J_1(\alpha(\phi_l))}{\alpha(\phi_l)} + \left(1 - \frac{1}{K}\right) \\
&\quad \times\left(\frac{2J_1(\alpha(\phi_l-\phi_\bullet))}{\alpha(\phi_l-\phi_\bullet)}\cdot\frac{2J_1(\alpha(\phi_\bullet))}{\alpha(\phi_\bullet)}\right).
\end{aligned} \tag{97}$$

It follows from (94) and (97) that

$$\begin{aligned}\mathrm{E}_{\mathbf{z}}\{\eta_2\} &= \frac{1}{K}\sum_{l=1}^{L}[\bar{\mathbf{E}}^{-1}\bar{\mathbf{g}}_0]_l \cdot \frac{2J_1(\alpha(\phi_l))}{\alpha(\phi_l)} + \left(1-\frac{1}{K}\right) \\ &\quad \times \left(\frac{2J_1(\alpha(\phi_\bullet))}{\alpha(\phi_\bullet)}\sum_{l=1}^{L}[\bar{\mathbf{E}}^{-1}\bar{\mathbf{g}}_0]_l \cdot \frac{2J_1(\alpha(\phi_l-\phi_\bullet))}{\alpha(\phi_l-\phi_\bullet)}\right) \\ &= \frac{1}{K}\sum_{l=1}^{L}[\bar{\mathbf{E}}^{-1}\bar{\mathbf{g}}_0]_l \cdot [\bar{\mathbf{g}}_0]_l + \left(1-\frac{1}{K}\right) \\ &\quad \times \left(\frac{2J_1(\alpha(\phi_\bullet))}{\alpha(\phi_\bullet)}\sum_{l=1}^{L}[\bar{\mathbf{E}}^{-1}\bar{\mathbf{g}}_0]_l \cdot [\bar{\mathbf{g}}_{\phi_\bullet}]_l\right) \\ &= \frac{1}{K}\bar{\mathbf{g}}_0^T\bar{\mathbf{E}}^{-1}\bar{\mathbf{g}}_0 \\ &\quad + \left(1-\frac{1}{K}\right)\left(\frac{2J_1(\alpha(\phi_\bullet))}{\alpha(\phi_\bullet)}\cdot\bar{\mathbf{g}}_0^T\bar{\mathbf{E}}^{-1}\bar{\mathbf{g}}_{\phi_\bullet}\right).\end{aligned} \tag{98}$$

Now, let us turn our attention to obtaining $\mathrm{E}_{\mathbf{z}}\{\eta_3\}$. Using the definition of $\mathbf{A}$ in (90), it follows that

$$\begin{aligned}\eta_3 &= \frac{1}{K^2}\sum_{l=1}^{L}\sum_{p=1}^{L}[\bar{\mathbf{E}}^{-1}\bar{\mathbf{g}}_0]_l[\bar{\mathbf{E}}^{-1}\bar{\mathbf{g}}_0]_p\mathbf{a}_{\phi_\bullet}^H\mathbf{a}_{\phi_l}\mathbf{a}_{\phi_p}^H\mathbf{a}_{\phi_\bullet} \qquad (99)\\ &= \sum_{l=1}^{L}[\bar{\mathbf{E}}^{-1}\bar{\mathbf{g}}_0]_l[\bar{\mathbf{E}}^{-1}\bar{\mathbf{g}}_0]_l\theta_l^{(2)} \\ &\quad + \sum_{l=1}^{L}\sum_{\substack{p=1\\p\neq l}}^{L}[\bar{\mathbf{E}}^{-1}\bar{\mathbf{g}}_0]_l[\bar{\mathbf{E}}^{-1}\bar{\mathbf{g}}_0]_p\theta_{l,p}^{(3)} \qquad (100)\end{aligned}$$

where

$$\theta_l^{(2)} \triangleq \frac{1}{K^2}\mathbf{a}_{\phi_\bullet}^H\mathbf{a}_{\phi_l}\mathbf{a}_{\phi_l}^H\mathbf{a}_{\phi_\bullet} \tag{101}$$

$$\theta_{l,p}^{(3)} \triangleq \frac{1}{K^2}\mathbf{a}_{\phi_\bullet}^H\mathbf{a}_{\phi_l}\mathbf{a}_{\phi_p}^H\mathbf{a}_{\phi_\bullet}. \tag{102}$$

It is direct to observe that the RHS of (101) may be obtained by substituting $\mathbf{a}_{\phi_l}$ in lieu of $\mathbf{a}_0$ in the RHS of (88). This similarity between $\theta_l^{(2)}$ and $\eta_1$ can be exploited to derive a more concise from of $\theta_l^{(2)}$ and $\mathrm{E}_{\mathbf{z}}\{\theta_l^{(2)}\}$ from (92) and (93), respectively. We have

$$\begin{aligned}\theta_l^{(2)} &= \frac{1}{K^2}\sum_{k=1}^{K}\sum_{s=1}^{K}e^{j\alpha(\phi_l-\phi_\bullet)z_k}e^{-j\alpha(\phi_l-\phi_\bullet)z_s} \\ &= \frac{1}{K} + \frac{1}{K^2}\sum_{k=1}^{K}e^{j\alpha(\phi_l-\phi_\bullet)z_k}\sum_{\substack{s=1\\s\neq k}}^{K}e^{-j\alpha(\phi_l-\phi_\bullet)z_s}\end{aligned} \tag{103}$$

and

$$\mathrm{E}_{\mathbf{z}}\left\{\theta_l^{(2)}\right\} = \frac{1}{K} + \left(1-\frac{1}{K}\right)\left(\frac{2J_1(\alpha(\phi_l-\phi_\bullet))}{\alpha(\phi_l-\phi_\bullet)}\right)^2 \tag{104}$$

or, equivalently,

$$\mathrm{E}_{\mathbf{z}}\left\{\theta_l^{(2)}\right\} = \frac{1}{K}[\bar{\mathbf{E}}]_{ll} + \left(1-\frac{1}{K}\right)[\bar{\mathbf{g}}_{\phi_\bullet}]_l[\bar{\mathbf{g}}_{\phi_\bullet}]_l. \tag{105}$$

Similarly, the RHS of (102) is obtained by substituting $\mathbf{a}_{\phi_p}$ in lieu of $\mathbf{a}_0$ in the RHS of (95). Making the same substitution in the RHSs of (96) and (97), we obtain

$$\begin{aligned}\theta_{l,p}^{(3)} &= \frac{1}{K^2}\sum_{k=1}^{K}e^{j\alpha(\phi_l-\phi_p)z_k} \\ &\quad + \frac{1}{K^2}\sum_{k=1}^{K}e^{j\alpha(\phi_l-\phi_\bullet)z_k}\sum_{\substack{s=1\\s\neq k}}^{K}e^{j\alpha(\phi_\bullet-\phi_p)z_s}\end{aligned} \tag{106}$$

and

$$\begin{aligned}\mathrm{E}_{\mathbf{z}}\left\{\theta_{l,p}^{(3)}\right\} &= \frac{1}{K}\cdot\frac{2J_1(\alpha(\phi_l-\phi_p))}{\alpha(\phi_l-\phi_p)} + \left(1-\frac{1}{K}\right) \\ &\quad \times \left(\frac{2J_1(\alpha(\phi_l-\phi_\bullet))}{\alpha(\phi_l-\phi_\bullet)}\cdot\frac{2J_1(\alpha(\phi_\bullet-\phi_p))}{\alpha(\phi_\bullet-\phi_p)}\right)\end{aligned} \tag{107}$$

or, equivalently,

$$\mathrm{E}_{\mathbf{z}}\left\{\theta_{l,p}^{(3)}\right\} = \frac{1}{K}[\bar{\mathbf{E}}]_{pl} + \left(1-\frac{1}{K}\right)[\bar{\mathbf{g}}_{\phi_\bullet}]_l[\bar{\mathbf{g}}_{\phi_\bullet}]_p. \tag{108}$$

Taking the expectation operation from both sides of (100) and using (105) and (108) yields

$$\begin{aligned}\mathrm{E}_{\mathbf{z}}\{\eta_3\} &= \frac{1}{K}\sum_{l=1}^{L}[\bar{\mathbf{E}}^{-1}\bar{\mathbf{g}}_0]_l[\bar{\mathbf{E}}^{-1}\bar{\mathbf{g}}_0]_l[\bar{\mathbf{E}}]_{ll} \\ &\quad + \left(1-\frac{1}{K}\right)\sum_{l=1}^{L}[\bar{\mathbf{E}}^{-1}\bar{\mathbf{g}}_0]_l[\bar{\mathbf{E}}^{-1}\bar{\mathbf{g}}_0]_l[\bar{\mathbf{g}}_{\phi_\bullet}]_l[\bar{\mathbf{g}}_{\phi_\bullet}]_l \\ &\quad + \frac{1}{K}\sum_{l=1}^{L}\sum_{\substack{p=1\\p\neq l}}^{L}[\bar{\mathbf{E}}^{-1}\bar{\mathbf{g}}_0]_l[\bar{\mathbf{E}}^{-1}\bar{\mathbf{g}}_0]_p[\bar{\mathbf{E}}]_{pl} \\ &\quad + \left(1-\frac{1}{K}\right)\sum_{l=1}^{L}\sum_{\substack{p=1\\p\neq l}}^{L}[\bar{\mathbf{E}}^{-1}\bar{\mathbf{g}}_0]_l[\bar{\mathbf{E}}^{-1}\bar{\mathbf{g}}_0]_p[\bar{\mathbf{g}}_{\phi_\bullet}]_l[\bar{\mathbf{g}}_{\phi_\bullet}]_p \\ &= \frac{1}{K}\sum_{l=1}^{L}\sum_{p=1}^{L}[\bar{\mathbf{E}}^{-1}\bar{\mathbf{g}}_0]_l[\bar{\mathbf{E}}^{-1}\bar{\mathbf{g}}_0]_p[\bar{\mathbf{E}}]_{pl} \\ &\quad + \left(1-\frac{1}{K}\right)\sum_{l=1}^{L}\sum_{p=1}^{L}[\bar{\mathbf{E}}^{-1}\bar{\mathbf{g}}_0]_l[\bar{\mathbf{E}}^{-1}\bar{\mathbf{g}}_0]_p[\bar{\mathbf{g}}_{\phi_\bullet}]_l[\bar{\mathbf{g}}_{\phi_\bullet}]_p \\ &= \frac{1}{K}\bar{\mathbf{g}}_0^T\bar{\mathbf{E}}^{-1}\bar{\mathbf{g}}_0 + \left(1-\frac{1}{K}\right)\left(\bar{\mathbf{g}}_0^T\bar{\mathbf{E}}^{-1}\bar{\mathbf{g}}_{\phi_\bullet}\right)^2.\end{aligned} \tag{109}$$

Substituting (93), (98), and (109) into (91), (35) follows. Let us now turn our attention to proving (37). Equation (25) can be used in (88) to show that

$$\lim_{K\to\infty}\eta_1 \xrightarrow{p1} \left(\frac{2J_1(\alpha(\phi_\bullet))}{\alpha(\phi_\bullet)}\right)^2. \tag{110}$$

Similarly, using (25) in (95), we obtain

$$\begin{aligned}\lim_{K\to\infty}\theta_l^{(1)} &\xrightarrow{p1} \frac{2J_1(\alpha(\phi_\bullet))}{\alpha(\phi_\bullet)}\cdot\frac{2J_1(\alpha(\phi_l-\phi_\bullet))}{\alpha(\phi_l-\phi_\bullet)} \\ &= \frac{2J_1(\alpha(\phi_\bullet))}{\alpha(\phi_\bullet)}\cdot[\bar{\mathbf{g}}_{\phi_\bullet}]_l.\end{aligned} \tag{111}$$

It directly follows from (94) and (111) that

$$\lim_{K\to\infty} \eta_2 \xrightarrow{p1} \frac{2J_1(\alpha(\phi_\bullet))}{\alpha(\phi_\bullet)} \cdot \bar{\mathbf{g}}_0^T \bar{\mathbf{E}}^{-1} \bar{\mathbf{g}}_{\phi_\bullet}. \tag{112}$$

Finally, using (25) in (99), it can be readily shown that

$$\lim_{K\to\infty} \eta_3 \xrightarrow{p1} \left(\bar{\mathbf{g}}_0^T \bar{\mathbf{E}}^{-1} \bar{\mathbf{g}}_{\phi_\bullet}\right)^2.$$

Considering (87) as $K \to \infty$ and using (110), (112), and (113), (37) follows. This completes the proof.

## REFERENCES


[1] H. Ochiai, P. Mitran, H. V. Poor, and V. Tarokh, "Collaborative beamforming for distributed wireless ad hoc sensor networks," *IEEE Trans. Signal Process.*, vol. 53, pp. 4110–4124, Nov. 2005.

[2] M. F. A. Ahmed and S. A. Vorobyov, "Collaborative beamforming for wireless sensor networks with Gaussian distributed sensor nodes," *IEEE Trans. Wireless Commun.*, pp. 638–643, Feb. 2009.

[3] L. Dong, A. P. Petropulu, and H. V. Poor, "A cross-layer approach to collaborative beamforming for wireless ad hoc networks," *IEEE Trans. Signal Process.*, vol. 56, pp. 2981–2993, Jul. 2008.

[4] K. Zarifi, S. Affes, and A. Ghrayeb, "Distributed beamforming for wireless sensor networks with random node location," presented at the Int. Conf. Acoustics, Speech, and Signal Process. (ICASSP), Taipei, Taiwan, Apr. 2009.

[5] C.-W. Chang, A. Kothari, A. Jafri, D. Koutsonikolas, D. Peroulis, and Y. C. Hu, "Radiating sensor selection for distributed beamforming in wireless sensor networks," presented at the IEEE Military Commun. Conf. (MILCOM), San Diego, CA, Nov. 2008.

[6] R. Mudumbai, G. Barriac, and U. Madhow, "On the feasibility of distributed beamforming in wireless sensor networks," *IEEE Trans. Wireless Commun.*, vol. 6, pp. 1754–1763, May 2007.

[7] D. R. Brown III and H. V. Poor, "Time-slotted round-trip carrier synchronization for distributed beamforming," *IEEE Trans. Signal Process.*, vol. 56, pp. 5630–5643, Nov. 2008.

[8] J. A. Bucklew and W. A. Sethares, "Convergence of a class of decentralized beamforming algorithms," *IEEE Trans. Signal Process.*, vol. 56, pp. 2280–2288, Jun. 2008.

[9] A. G. Marques, X. Wang, and G. B. Giannakis, "Minimizing transmit power for coherent communications in wireless sensor networks with finite-rate feedback," *IEEE Trans. Signal Process.*, vol. 56, pp. 4446–4457, Sep. 2008.

[10] M. M. Abdallah and H. C. Papadopoulos, "Beamforming algorithms for information relaying in wireless sensor networks," *IEEE Trans. Signal Process.*, vol. 56, pp. 4772–4784, Oct. 2008.

[11] V. Havary-Nassab, S. Shahbazpanahi, A. Grami, and Z.-Q. Luo, "Distributed beamforming for relay networks based on second-order statistics of the channel state information," *IEEE Trans. Signal Process.*, vol. 56, pp. 4306–4316, Sep. 2008.

[12] R. Mudumbai, D. R. Brown, U. Madhow, and H. V. Poor, "Distributed transmit beamforming: Challenges and recent progress," *IEEE Commun. Mag.*, vol. 47, pp. 102–110, Feb. 2009.

[13] H. Steyskal, R. A. Shore, and R. L. Haupt, "Methods for null control and their effects on radiation pattern," *IEEE Trans. Antennas Propag.*, vol. 34, pp. 404–409, Mar. 1986.

[14] B. Friedlander and B. Porat, "Performance analysis of a null-steering algorithm based on direction-of-arrival estimation," *IEEE Trans. Signal Process.*, vol. 37, pp. 461–466, Apr. 1989.

[15] L. C. Godara, "Application of antenna arrays to mobile communications, Part II: Beam-forming and direction-of-arrival considerations," *Proc. IEEE*, vol. 85, pp. 1195–1245, Aug. 1997.

[16] A. Perez-Neira, X. Mestre, and J. R. Fonollosa, "Smart antennas in software radio base stations," *IEEE Commun. Mag.*, vol. 39, pp. 166–173, Feb. 2001.

[17] J. A. Stine, "Exploiting smart antennas in wireless mesh networks using contention access," *IEEE Wireless Commun.*, vol. 13, pp. 38–49, Apr. 2006.

[18] J. Mar and Y.-R. Lin, "Implementation of SDR digital beamformer for microsatellite SAR," *IEEE Geosci. Remote Sens. Lett.*, vol. 6, pp. 92–96, Jan. 2009.

[19] P. Gupta and P. R. Kumar, "Critical power for asymptotic connectivity in wireless networks," in *Stochastic Analysis, Control, Optimization and Applications: A Volume in Honor of W. H. Fleming*, W. M. McEneany, G. Yin, and Q. Zhang, Eds. Boston, MA: Birkhauser, 1998, pp. 547–566.

[20] M. Haenggi, "On distances in uniformly random networks," *IEEE Trans. Inf. Theory*, vol. 51, pp. 3584–3586, Oct. 2005.

[21] S. Mukherjee, D. Avidor, and K. Hartman, "Connectivity, power, and energy in a multihop cellular-packet system," *IEEE Trans. Veh. Technol.*, vol. 56, pp. 818–836, Mar. 2007.

[22] W. Wang, V. Srinivasan, and K.-C. Chua, "Coverage in hybrid mobile sensor networks," *IEEE Trans. Mobile Comput.*, vol. 7, pp. 1374–1387, Nov. 2008.

[23] A. Paulraj and T. Kailath, "Eigenstructure methods for direction of arrival estimation in the presence of unknown noise fields," *IEEE Trans. Acoust. Speech Signal Process.*, vol. 34, pp. 13–20, Feb. 1986.

[24] S. Affes, S. Gazor, and Y. Grenier, "An algorithm for multisource beamforming and multitarget tracking," *IEEE Trans. Signal Process.*, vol. 44, pp. 1512–1522, Jun. 1996.

[25] H. Li, P. Stoica, and J. Li, "Computationally efficient maximum likelihood estimation of structured covariance matrices," *IEEE Trans. Signal Process.*, vol. 47, pp. 1314–1323, May 1999.

[26] S. A. Vorobyov, A. B. Gershman, and Z.-Q. Luo, "Robust adaptive beamforming using worst-case performance optimization: A solution to the signal mismatch problem," *IEEE Trans. Signal Process.*, vol. 51, pp. 313–324, Feb. 2003.

[27] A. Hjørungnes, D. Gesbert, and J. Akhtar, "Precoding of space-time block coded signals for joint transmit-receive correlated MIMO channels," *IEEE Trans. Wireless Commun.*, vol. 5, pp. 492–497, Mar. 2006.

[28] B. Friedlander, "Communications through time-varying subspace channels," *IEEE J. Sel. Areas Commun.*, vol. 26, pp. 338–347, Feb. 2008.

[29] X. Gao, B. Jiang, X. Li, A. B. Gershman, and M. R. McKay, "Statistical eigenmode transmission over jointly correlated MIMO channels," *IEEE Trans. Inf. Theory*, vol. 55, pp. 3735–3750, Aug. 2009.

[30] R. H. Gohary and T. N. Davidson, "On rate-optimal MIMO signalling with mean and covariance feedback," *IEEE Trans. Wireless Commun.*, vol. 8, pp. 912–921, Feb. 2009.


**Keyvan Zarifi** (S'04–M'08) received the Ph.D. degree (with the highest honors) in electrical and computer engineering from Darmstadt University of Technology, Darmstadt, Germany, in 2007.

From January 2002 until March 2005, he was with the Department of Communication Systems, University of Duisburg-Essen, Duisburg, Germany. From April 2005 until September 2007, he was with the Darmstadt University of Technology. From September 2002 until March 2003, he was a visiting scholar at the Department of Electrical and Computer Engineering, McMaster University, Hamilton, Ontario, Canada. Since September 2007, he has been jointly with Institut National de la Recherche Scientifique-Énergie, Matériaux, et Télécommunications (INRS-EMT), Université du Québec, and Concordia University, Montreal, Quebec, Canada, as a Postdoctoral Fellow. His research interests include statistical signal processing, wireless sensor networks, MIMO and cooperative communications, and blind estimation and detection techniques.

In 2008, Mr. Zarifi received a Postdoctoral Fellowship from the Natural Sciences and Engineering Research Council of Canada (NSERC).

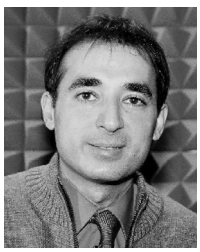

**Sofiène Affes** (S'94–M'95–SM'04) received the Diploma d'Ingénieur in telecommunications in 1992 and the Ph.D. degree with honors in signal processing in 1995, both from the École Nationale Supérieure des Télécommunications (ENST), Paris, France.

He has been since with INRS-EMT, University of Quebec, Montreal, Canada, as a Research Associate from 1995 until 1997, as an Assistant Professor until 2000, then as an Associate Professor until 2009. Currently he is a Full Professor in the Wireless Communications Group. His research interests are in wireless communications, statistical signal and array processing, adaptive space-time processing and MIMO.

From 1998 to 2002 he was leading the radio design and signal processing activities of the Bell/Nortel/NSERC Industrial Research Chair in Personal Communications at INRS-EMT, Montreal, Canada. Since 2004, he has been actively involved in major projects in wireless of PROMPT (Partnerships for Research on Microelectronics, Photonics and Telecommunications).

Prof. Affes was the co-recipient of the 2002 Prize for Research Excellence of INRS. He currently holds a Canada Research Chair in Wireless Communications and a Discovery Accelerator Supplement Award from NSERC (Natural Sciences and Engineering Research Council of Canada). In 2006, he served as a General Co-Chair of the IEEE VTC'2006-Fall conference, Montreal, Canada. In 2008, he received from the IEEE Vehicular Technology Society the IEEE VTC Chair Recognition Award for exemplary contributions to the success of IEEE VTC. He currently acts as a member of the Editorial Board of the IEEE TRANSACTIONS ON WIRELESS COMMUNICATIONS and of the Wiley *Journal on Wireless Communications and Mobile Computing*.

**Ali Ghrayeb** (S'97–M'00–SM'06) received the Ph.D. degree in electrical engineering from the University of Arizona, Tucson, in 2000.

He is currently an Associate Professor with the Department of Electrical and Computer Engineering, Concordia University, Montreal, QC, Canada. He holds a Concordia University Research Chair in Wireless Communications. He is the coauthor of the book *Coding for MIMO Communication Systems* (Wiley, 2008). His research interests include wireless and mobile communications, error correcting coding, MIMO systems, wireless cooperative networks, and CDMA/WCDMA systems.

Dr. Ghrayeb has instructed/co-instructed technical tutorials at several major IEEE conferences. He serves as an Associate Editor of the IEEE TRANSACTIONS ON VEHICULAR TECHNOLOGY and IEEE TRANSACTIONS ON SIGNAL PROCESSING. He served as an Associate Editor of the Wiley *Wireless Communications and Mobile Computing Journal* from 2004 to 2008.